NICI

Near Infrared Coronagraphic Imager

Operational Concepts Definition Document

CDR Version

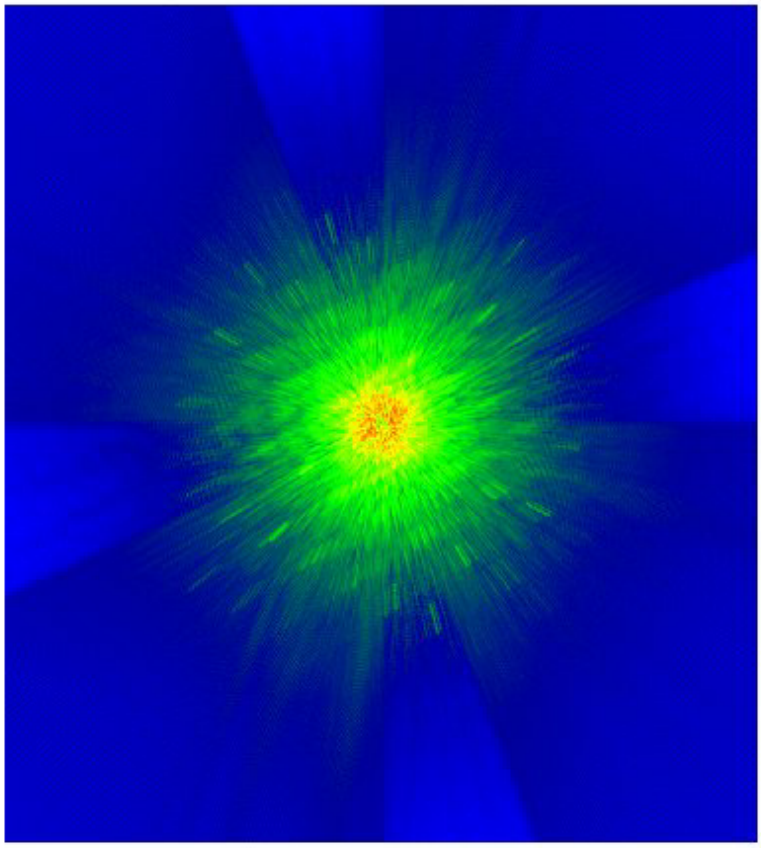

June 10, 2002

Mauna Kea Infrared

Table of Contents

1. Introduction

1.1. The Purpose of this Document

The purpose of this document is to provide an overview of the Near Infrared Coronagraphic Imager (NICI), delineating what the instrument can do and how observers can use it. This document starts with a summary of the targeted science, a description of the science derived requirements, and the instrument requirements. An overview of instrument hardware and software is given to provide context for the final section of observer operations in detail.

1.2. Purpose of the Instrument

We stand on the brink of a new understanding of the Universe and of our place in it. After centuries of debate, speculation, and rhetoric, and after many false starts and erroneous claims, in our lifetimes, a population of objects has been reliably and repeatably identified as extra solar planets. In addition to these exciting and fundamental observations, we have obtained a few glimpses into the intermediate stages that link the birth of stars to the formation of planetary systems. We are poised now for the transition from discovery of these systems to their characterization. Our tools are marshaled for this transition. On the ground we have a new generation of large aperture telescopes equipped with advanced detectors, and the atmospheric compensation systems needed to achieve diffraction limited imaging. In space we have established a major working observatory and have programs in various stages of completion to follow it with missions that will have even larger apertures, longer wavelength infrared imaging and higher astrometric accuracy. In the years to come there will be a significant array of instrumentation dedicated to the exploration and understanding of extra solar planetary systems.

In this document we describe a unique addition to this campaign. It is an imaging facility instrument, yet it has a narrowly focused purpose. From the very beginning, its design has been optimized to address this purpose with little compromise. Its goal is to extend our insight into the nature of this newly discovered planetary population by enabling deep imaging in circumstellar halo. This capability nicely complements the bias of radial velocity investigations for systems with high orbital velocities, highly inclined orbital planes, and periods not significantly exceeding the duration of the experiment. Moreover, it will be sensitive to symmetrically distributed material, disks characteristic of the emergence of young stellar objects, and the formation of mature planetary systems.

The NICI instrument design emerged from the desire to accomplish a compelling body of scientific inquiry. As a group, they have a common theme: the investigation of phenomena that occur in the immediate vicinity of some much brighter central source. Given that the vast majority of the night sky does not fall into this category, it may seem wasteful to build an instrument just to study these few square arc seconds. Indeed, almost all imaging instruments, particularly facility class instruments tend, if anything, to

sacrifice sampling for field of view. We know, however, that the circumstellar environment is the key to the study of a host of important astronomical phenomena either because, like planet formation, they only take place in the circumstellar environment or, like the host galaxies of QSOs, they can tell us much about the central object itself.

Deep imaging in the circumstellar region is not a new problem. The science goals of the Large Space Telescope program (c.f. Spitzer, 1978) were as much about the decreased image sidelobes of the telescope and circumstellar science as they were about the compact core of the PSF. It is only recently, however, that technical advances like large area infrared arrays and adaptive optics systems, and institutional focus like the NASA Origins and NSF/NASA NStars programs have combined to enable realization of a dedicated circumstellar imaging campaign. This instrument is one element of that campaign.

2. Targeted Science Overview

2.1. Coronagraphic Imaging

Each astronomical instrument spans some domain of observational parameter space over which it can make useful observations. Experience has consistently shown that opening new windows into that space yields new and unanticipated science. Traditional venues for instrumental advances have involved enhanced sensitivity, or new domains of spatial and/or spectral resolution. In this proposal, however, we describe an instrument designed to explore a new part of the sky, a region that has remained largely unobserved by direct means at any wavelength. The target is the halo region immediately surrounding the image of any source.

The few square arc seconds of the circumstellar halo occupy a small fraction of the sky, yet the halo region is disproportionately rich with astronomical importance and potential. It is here that the study of the circumstellar environment, from stellar birth to formation of mature planetary systems, lies hidden. It is here that the search for sub-stellar companions, brown dwarfs, and extra solar planets must proceed. And it is here, also, that the nature of the central regions of active galactic nuclei remains hidden. From our nearest neighbor stars to the brightest, most distant known objects, there is important science hidden beneath the glare of the circumstellar halo.

From the nearest stars to the furthest quasars, there are a host of significant astronomical questions that would also benefit from deep circumstellar imaging. For example, the nature of the low-mass end of the initial stellar mass function, and consequently the baryonic contribution to the mass of the universe, relies on characterizing the mass and distribution of brown dwarfs. If, as seems to be the case, stellar multiplicity extends to the brown dwarf population, then brown dwarfs in multiple systems could easily be under sampled. The evolution of close binary systems, and the behavior of novae and supernovae could likewise be studied by deep imaging in the circumstellar region. The stellar halo can also become a significant factor in studying crowded fields like globular clusters, where the accumulated halos of many bright stars in the field can mask fainter sources. Similarly, the integrated point source halos of an

extended object can prevent imaging fainter sources, as in the case of satellites near a planetary limb.

The detection and characterization of extra solar planetary system is, in many ways, the archetypal circumstellar imaging problem, and is a fundamental piece of the search for who and what we are as a species. Ultimately, we wish to understand the frequency and nature of intelligent life in the universe, but there are significant gaps in our basic understanding of planetary systems. How are planets made and how are planet and star formation related? In what ways is the solar system typical or atypical of planetary systems? What determines where and if planets of a given type form, and where in the system they are ultimately observed? All phases of the evolution of planetary systems, from stellar birth to maturity, can be investigated via deep circumstellar imaging. The list of questions is long and the program to answer them difficult and exciting. Many disciplines and instruments will be brought to bear on this problem, but imaging has always played a special role in the planetary community and is vital for separating stellar from circumstellar light.

In exploring the circumstellar environment, the stellar coronagraph has become the instrument of choice. It has become closely identified with the search for sub-stellar companions. Like Gemini, many of the world's major telescope programs have either built or planned a similar instrument. Two were added to the Hubble Space Telescope (STIS and NICMOS) and one has been built into the Advanced Camera for Surveys. These coronagraphs, however, were all designed as “add-ons” to an instrument designed and built to accomplish different science goals.

The coronagraph is indeed a powerful instrument, but the nature of that power has been largely misunderstood, partly because its action is governed by diffractive rather than geometric optics, but mostly because it is primarily an enabling instrument, particularly in ground-based systems. It cannot by itself, detect planets. When designed and used properly, it should allow the observer to achieve the long integrations and the accurate background subtractions needed to image at high dynamic range. Ultimately, as with any instrument, it is the skill of the observer in taking and reducing data that will determine the performance level of the instrument.

2.2. Origins and Coronagraphic Imaging

One of the earliest published references to the use of a coronagraph for a purpose other than observing the Sun was a paper on extra solar planet detection (Kenknight 1977). The suggestion was made to use a coronagraph for the detection of planets around other stars. In some sense, the close association of coronagraphic imaging with Origins Science began with this paper. The exciting discovery of a protoplanetary disk around the Star β-Pictoris (Smith and Terrile, 1984) crystallized the high level of interest in this kind of science and once again drew attention to the value of the coronagraph as a scientific tool. Reports from many review panels (c.f. Burke, 1992 and Elachi et. al., 1996) have stressed the importance of both the Origins Science program and the value of direct imaging to that effort. Those early reports focused primarily on the space-based imaging program because of the general impression that the turbulent atmosphere represented a fundamental limit to deep imaging. The atmosphere certainly remains an

obstacle, but what true limit to imaging it represents is no longer clear. There are new telescopes and new technologies, but most of all there is human invention. The limit to what can be done from the ground has yet to be defined.

The present instrument is a milestone in circumstellar science. It is the first instrument to be designed solely for that purpose. It will be the only instrument of its kind to operate at a large telescope and be completely self-contained, with only the telescope between it and the sky. It is only fitting that it is driven by an ambitious and open-ended scientific agenda, and that it be designed to enable that human invention to the highest degree possible.

2.3. Young Stellar Objects

How stars and planetary systems form is one of the fundamental questions posed by NASA's Origins Program. Since protoplanetary disks form in the environments of Young Stellar Objects (YSOs), studies of the evolution and diversity of YSOs are essential to understanding the origin of planetary systems. There are regions in YSOs where key physical processes occur that shape the formation and evolution of stars and planets. Detection, resolution, and characterization of these regions will help answer many important questions.

The current paradigm for the birth of low mass stars (Adams, Lada and Shu 1987) is largely based on the interpretation of spectral energy distributions (SEDs) from near-IR to millimeter wavelengths. In the earliest stages, the in-falling, dusty molecular envelopes surrounding embedded protostars are completely opaque at wavelengths shorter than about 25 microns. This is known as a Class 0 SED. Within the infalling envelope, a star and nebular disk form. Most of the material destined for the star first falls onto the disk where it dissipates angular momentum and accretes onto the star. While gas is falling onto the star, an accretion-driven stellar or disk wind develops, which begins to clear envelope gas away from the rotational poles of the star-disk system, terminating the growth of the disk, and possibly establishing the eventual mass of the star as well. This is the embedded YSO stage, with a Class I SED, characterized by a spectrum that rises beyond two microns because almost all the light from the star is absorbed and reradiated by circumstellar dust at long wavelengths. In the most deeply embedded objects, most of the scattered light may come from walls of the outflow cavity in the envelope, giving a comet-like appearance to the circumstellar reflection nebulosity. The Class I stage is thought to last for at least a few times 10^5 years.

The in-falling envelope disperses, leaving an optically visible classical T-Tauri star (CTTS) with a circumstellar disk. Accretion through the disk slows as the star gains the final few percent of its mass. This Class II stage lasts from $10^6 - 10^7$ years, and is characterized by a spectrum that has IR emission in excess of photospheric values, but that is constant or falling longward of two microns. Accretion through the disk finally ends, due to lack of replenishment or disk gaps created by planet formation. The disk becomes optically thin, and the system evolves into a weak-line T Tauri star (WTTS). This stage is classified as Class III. If an optically thin protoplanetary or planetary debris disk remains, the stellar spectrum is that of a stellar photosphere with a small amount of mid- and far-IR excess arising from the disk. Since the IR emission from these disks is

below the IRAS detection limits for nearby star-forming regions, there are currently only loose constraints on the timescale for dispersal of debris disks.

High-resolution near-IR (NIR) imaging of the circumstellar environments of YSOs complements information derived from SED modeling. It can provide direct observational confirmation at spatial scales that distinguish the morphology of circumstellar material spanning the full range of evolutionary states (ages $10^5 - 10^7$ yr). With improvements in infrared instrumentation and telescope thermal control, and with the arrival of AO-correction on 8m-class telescopes, ground-based NIR imaging can achieve 0.06 arcsec diffraction-limited imaging at 2.2 microns, while observations with WFPC2 and NICMOS on HST achieve far-optical and NIR resolutions of 0.1 and 0.2 arcsec respectively. At these resolutions, structures as small as eight AU can be resolved in Taurus-Auriga (140 pc) and ρ-Ophiuchus (125 pc), the two nearest and best-studied star-forming regions. (See, for example, HST imaging by Padgett et al. 1999, and AO-corrected NIR imaging by Close et al. 1997).

From these studies, a consistent picture of YSO structure is beginning to emerge. Many Class I and Class II YSOs appear as conical-to-parabolic reflection nebulae crossed by dark lanes. The dark lanes are identified as circumstellar disks that currently are best seen edge-on, and which extend at right angles to known optical, NIR, and millimeter outflows in these objects. Bipolar reflection nebulae are identified as the in-falling envelopes illuminated by the central stars and, in some cases, the top and bottom surfaces of optically thick circumstellar disks. Typically, the envelopes have diameters of about 1000AU, and the disks have lengths of about 500AU with apparent thickness of order 100AU. These widths define surfaces with NIR optical depths of one, rather than the actual scale height.

The limb-brightened cavities seen in some objects are probably boundaries between the in-falling envelope and accretion-driven outflow (Figure 2-1). If so, the large opening angles of the cavities are in contrast to the narrowly collimated jets observed within the cavities of some objects. HH 30 in the Taurus molecular cloud (distance 140 pc) is the textbook example of a jet emerging from a YSO viewed edge-on. In this orientation, the problem of a bright central object is avoided because the disk itself occults it. Absent this effect, study of these disks at pole-on orientations is precluded. In the WFPC2 observations by Burrows et al. (1996), the emission-line jet is highly collimated and the FWHM of the unresolved jet is less than 20 AU (0.15 arcsec). It can be traced to within 30 AU of the obscured star. Its width is much narrower than the cleared cavity, so collimation must occur much closer to the star, in a region that is obscured by the edge-on disk. No-mask coronagraphic modes in NICI will permit imaging much closer to star.

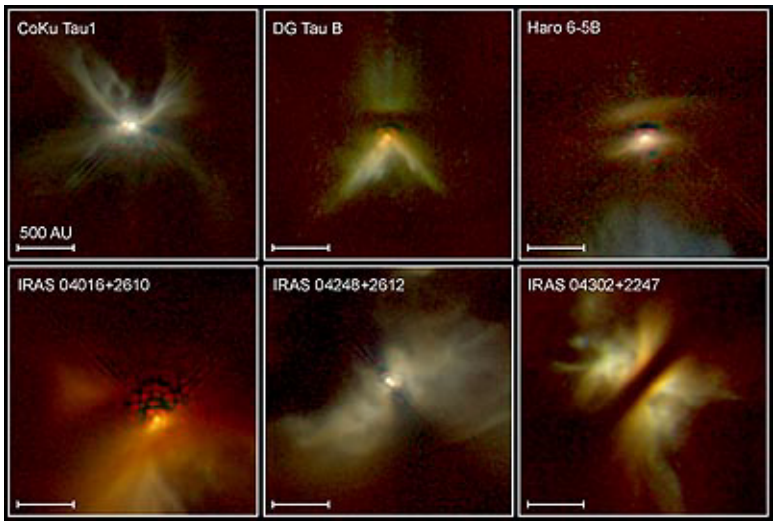

Figure 2-1 HST-Nicmos images of young stellar disks.

NICI will be a powerful tool for probing the in-falling envelopes, disks, and jets of YSOs. Diffraction-limited NIR imaging will resolve structures with scales of about eight AU in the ρ-Ophiuchus and R Coronae Australis molecular clouds, significantly better than that achieved by HST. Past high-resolution studies have selected edge-on YSOs to avoid scattered light problems. With coronagraphic rejection of light from the more pole-on YSOs, we will be able to obtain unbiased surveys of YSOs.

High spatial resolution and low background level will yield unprecedented information on the geometry and distribution of material in in-falling envelopes, the geometry and extent of wind-created cavities, and the distribution of material within disks, against which to test YSO models. Virtually no high resolution imaging of YSOs has been performed in the 3-5 micron region where we will obtain ten AU spatial resolutions on deeply embedded structures. High spatial resolution is crucial in order to probe regions ten AU from the stellar surface, where wind/cloud interactions may be revealed. Imaging in spectral lines that probe shocked gas (e.g. [FeII] at 1.64 microns and the 1-0 S(1) line of H_2 at 2.12 microns) will trace the highly collimated jets into the inner regions of accretion disks, perhaps revealing the collimating mechanism. Such observations are fundamental to understanding the role played by outflows in terminating infall, and perhaps determining stellar masses.

Jets contain knots, which are probably created by discrete accretion events from instabilities in the inner accretion disk. At high resolution, these knots will have significant proper motions. By measuring these proper motions, it should be possible to characterize the timescale of accretion instabilities in the disk, and thereby learn much about the physics of the accretion process. An even closer association of T Tauri stars has recently been identified in the vicinity of TW Hydrae (Kastner et al. 1997), which is

almost overhead at Gemini South. Given its proximity (55 pc), age (~10^7 yr) and abundance of binary systems, the TW Hya association is ideally suited to studies of diversity and evolution of circumstellar disks.

High-mass (OB) star formation is poorly understood. The formation of massive stars is not merely a scaled-up version of low mass star formation. Massive stars are rarer, disproportionately more luminous, evolve much faster, and are associated with much more violent events than their less massive counterparts, e.g. powerful bipolar jets and outflows, high velocity stellar winds, and supernova explosions. Because of the low probability of forming high mass stars and their extremely short evolutionary timescales (evolving off the main sequence in 10^7 yr) their space density is relatively low. Consequently, the closest massive stars are 450 pc away in the Orion Trapezium cluster. Even at these distances, the picture is complicated by confusion due to multiple sources. Through its high resolution and coronagraphic capability, NICI will be able to conduct high sensitivity searches for outflows and disks in the environs of young O stars and will elucidate formation mechanisms.

2.4. Circumstellar Disks

Circumstellar disks around main sequence stars are the evolved counterparts of disks around YSOs. It is these main sequence circumstellar disks that are the link between planetary system formation and what we know as current, evolved planetary systems like our own. Hence, near infrared coronagraphic studies of these main sequence debris disks will help provide the science link necessary to understand how evolved planetary systems arise, form, evolve and survive.

Main sequence circumstellar debris disks like the IRAS-discovered prototypes Vega and β Pic have been found to be common, occurring around at least 15% of nearby field stars of types A-K. Defining characteristics of these objects include low dust luminosity and optical depth, small gas/dust mass ratio such that dust dynamics are approximately Keplerian, and short dust lifetimes relative to star ages. The dust is clearly "second generation", i.e. not primordial but released from larger parent bodies such as asteroids or comets. Star age estimates indicate that many of these disks are a few x 10^7 to a few x 10^8 years old, corresponding to the hypothesized time span for construction and heavy bombardment of planets in our solar system.

It is important to point out that second generation material around a star indicates not only the existence of planetesimals, but also of larger masses capable of sending small bodies into fragmenting collisions and star-grazing orbits to release dust and gas. Our solar system (SS) is an example of an old main-sequence (MS) system containing second-generation dust. An external observer detecting the SS dust could thereby infer the existence of remnant planetesimals and their planetary perturbers.

Recent images of some of the famous CS debris systems show them to be disks with central gaps about the size of the planetary region of our solar system, as had been inferred previously. High-resolution imaging has revealed fine structure in some of the disks, offering further indirect evidence of the existence of planet masses. Of the prototype MS CS dust systems, only β Pic so far has detectable dust within the central

gap, with model temperatures up to at least 350 K (Fajardo-Acosta et al. 1993). As noted in section II.B.1, the warm grains in that system (Knacke et al.1993) and in the young main sequence system 51 Oph (Fajardo-Acosta et al. 1993) have partially crystalline silicate mineralogy.

Upper limits on the amount of warm dust around other stars (for example Vega, see Aumann et al. 1985) are generally high due to lack of spatial resolution and low contrast of dust flux to stellar photospheres at short IR wavelengths. Ground-based follow-up to IRAS (Aumann and Probst 1991) showed that few MS systems have significant amounts of warm (T > 150K) dust. Several such rare cases have been found and studied recently by Fajardo-Acosta et al. (1998) via mid-IR spectrophotometry. Mid-IR images of HR 4796A (Koerner et al. 1998; Jayawardhana et al. 1998) resolved a central warm dust population radiating at 200-400 K.

The present best photometric sensitivity at 12 and 25 μm to terrestrial-temperature dust around the nearest stars is a few hundred times the optical depth in the SS zodiacal cloud. High spatial resolution will be required for detection of inner-system dust at densities lower than the IRAS/ISO/SIRTF limits of a few hundred "zodis". The nearest stellar system, α Centauri, contains G and K MS stars, and should be an especially interesting target. Unfortunately, it is located at galactic latitude of only -0.7° and is seen against complex bright background. This is another situation in which high-resolution coronagraphic imaging by NICI could be employed fruitfully.

The brightness of a 0.3 AU-diameter patch of the SS zodiacal cloud would approximately equal that of Earth at both visual and IR wavelengths. It is estimated that warm dust at more than about 10x SS density would challenge detectability of Earth-like planets via planned space-based mid-IR interferometers like NASA's TPF (Beichman 1998). Since dense exozodi dust may block attempts to detect terrestrial planets around other stars, NICI can play a valuable role as a survey instrument, exploring the frequency of inner-system dust around nearby stars to newly sensitive limits. Ironically, these asymmetries and planetary wakes in dense exozodiacal clouds could themselves be used to infer masses and locations of embedded planets (Dermott et al. 1998).

Circumstellar disks around main sequence stars have been observed from the ground and from space using coronagraphs. The archetype circumstellar disk surrounds Beta Pictoris (Smith and Terrile 1984). Since then, disks around other younger main sequence stars have been imaged, including recent observations of HR4796A and HD141569 from Hubble Space Telescope (Augereau et al. 1999; Schneider et al. 1999, Weinberger et al. 1999). These stars are probably like β Pictoris, and their debris disks represent a middle stage between young protoplanetary disks and old, mature systems. Of particular import are the observations of circumstellar disks around stars with known extra solar planets (Trilling and Brown, 1998; Trilling et al. 2000).

These observed disks are all debris disks - the leftover remains of planetary system formation. In the cases of the stars with known extra solar planets, the debris disks resemble our own Solar System's Kuiper Belt, a ring of debris that surrounds the planets in our Solar System and represents the outer limit of constructive planet formation in the early days of our Solar System. By observing these debris disk remnants

of planetary system birth, we learn about how planets form - and, by comparison, how our own Solar System formed.

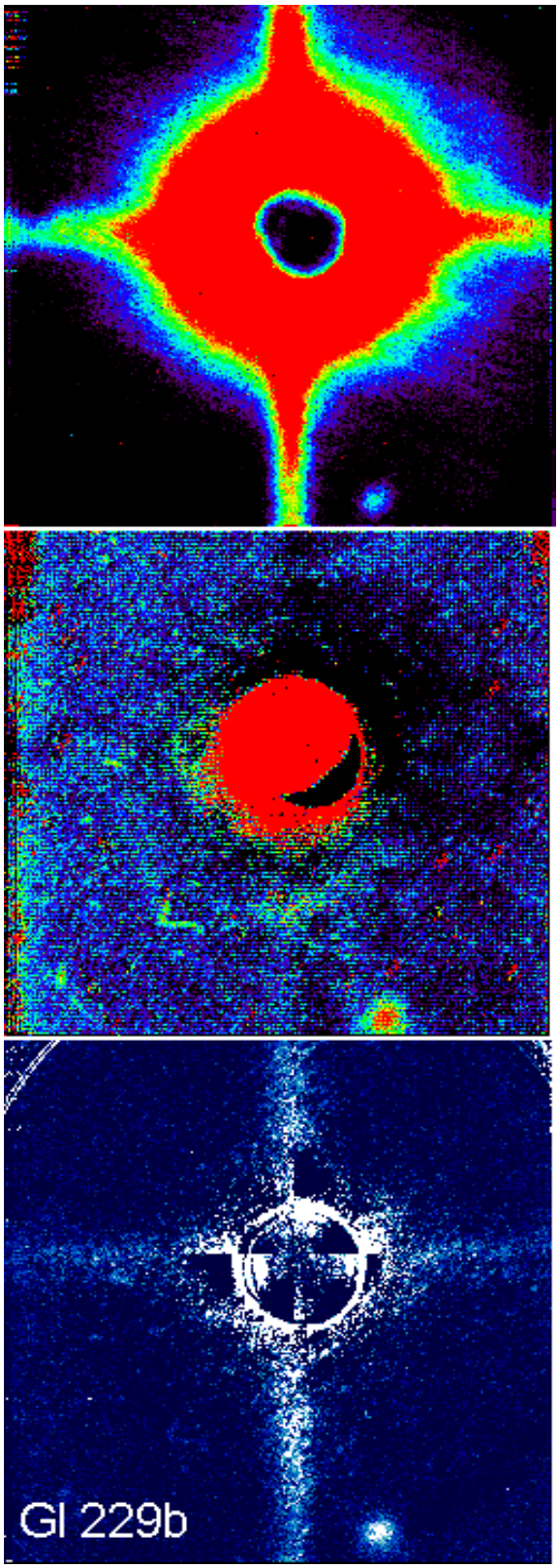

2.5. Brown Dwarf Observations: Multiplicity and the IMF

Binary star systems do not form in the same way that planetary systems do. Binary stars form from co-collapse of molecular clouds, as opposed to secondary collapse within a circumstellar disk. Thus, studying the multiplicity function of stars reveals information about a formation mechanism different from planetary system formation. Around half of all main sequence stars are in systems of multiplicity (binaries or higher) (Bodenheimer et al. 1993). Naturally, these multiplicities are imprinted signatures of stellar birth environments. However, it is unknown what the multiplicity is for main sequence stars with respect to brown dwarf sub-stellar companions. Additionally, the initial mass function (IMF, Scalo 1986, Meyer et al. 2000) below the edge of the main sequence has only recently begun to be defined, and more data is needed, especially at the lowest masses, to determine where the turnover in the initial mass function is. Thus, to study both the multiplicity of low mass companions as well as the mass function of low mass objects as companions requires the study of faint objects near bright objects, and therefore is an origins-oriented question in which NICI can directly participate.

Figure 2-2 GL229B taken at the IRTF with CoCo. The top image is a raw frame, the center is a methane-differenced frame and the lower one is a profile-differenced frame (See NRC Report: Failed Stars and Superplanets, 1998).

Brown dwarfs have been the subject of many papers in the topics of star and planet formation, the dark matter problem, and cosmology. Starting in 1995 (Teide 1, Rebolo et al. 1995; Gl 229 B, Nakajima et al. 1995), found once elusive objects to exist and that they may be numerous in the galaxy. This has raised many questions about their atmospheres, activity, weather, internal structure, evolution, and the sub-stellar Initial Mass Function (SIMF). The numbers of high mass BDs (75 to 40MJ) found in the field and in young open clusters and associations indicate that the IMF does not have a turnover at the sub-stellar limit (Martín et al. 1997a; Reid et al. 1999). However, theoretical models of star formation (e.g., Bodenheimer et al. 1993) have predicted that there has to be a minimum mass for fragmentation (e.g., Scalo 1988), which should imply a cutoff of the IMF below a certain mass. Such a minimum mass is very uncertain. Estimates have been made since the early 1970s, and they vary by two orders of magnitude from one tenth of a solar mass to about 1MJ. The fact that many field BDs have already been found effectively rules out minimum masses above the sub-stellar limit. An observational determination of the turnoff of the IMF will be a critical constraint for general models of star formation. If the SIMF extends to very low masses (~1MJ), this will significantly impact our understanding of giant planet formation. There will be two evolutionary paths, with distinctly different initial conditions, leading to essentially identical objects.

The first unambiguous detections of sub stellar low mass (brown dwarf) companions have only recently been made. The brown dwarf Gl229B was discovered (Nakajima et al. 1995) by direct imaging with a coronagraph working in visible light and follow up studies (c.f., Oppenheimer et al. 2000) have also been carried out with similar instruments. The cool spectrum of GL229B made visible detection relatively difficult from the point of view of high relative background levels. Follow up observations at the IRTF show that the object is relatively easily detected and its light easily isolated in the near infrared (Figure 2.2) by use of the cryogenic coronagraphic relay, CoCo (Wang et al 1994). Additionally, the study of stellar multiplicity can be extended to companions to sub stellar objects. Recently, Martín et al. (1999), Koerner et al. (1999), Basri and Martín (1999), Martín et al. (1998), among others, have found that the frequency of binarity in sub stellar objects may also be high. Martín et al. (2000) have found, using the adaptive optics system at the Keck telescope, that the Gl569 system has a very low mass companion binary (Gl569B and C) to the cool M star Gl569A, thus demonstrating that companions and multiplicity can be two sides of the same coin.

Low-mass BDs are incredibly faint and thus difficult to find, but younger ones are easier to see. Our best chance of finding low-mass BDs as companions is to search for them in young clusters and associations, or as companions to young stars, or even as companions to young BDs. (Note also that the radial velocity surveys do not study young active stars, so the multiplicity and number of companions to young stars is quite unknown.) Recently, an L dwarf has been identified in the young (~ 5My) open cluster Σ Ori (Zapatero-Osorio et al. 1999). Using recent evolutionary models that have been tested against the BD sequence of the Pleiades (Chabrier et al. 2000), a mass of order 15MJ was derived for it. If the SIMF of Σ Ori is typical of the Galactic disk, BDs exist down to at least 15 MJ, with an IMF slope rising at decreasing masses. The Deuterium-burning mass limit is at $13M_J$, so we are very close to crossing it in Σ Ori.

Radial velocity surveys have found a Brown Dwarf "Desert", i.e., an absence of BD companions to G and K-dwarf primaries within ~5AU (Marcy et al., 2000). On the other hand, BD companions to BD primaries appear to be relatively common. We know of the existence of one double-lined spectroscopic binary with BD components in the Pleiades (Basri and Martín 1999); and four binaries in the field where both components are ultra-cool dwarfs (Martín et al. 1999b, 2000a; Koerner et al. 1999). All of them have separations less than 10AU. The separation distribution of G and K dwarfs in the solar vicinity has a broad peak between 5 and 40 AU (Duquennoy and Mayor 1991). The mean orbital period is 180 years. However, BDs seem to prefer smaller separations. It is possible that planets around BDs also tend to be closer than planets around stars. There appears to be no prohibition against the formation of a small-scale solar system around BDs. The implication is that high angular resolution is extremely important for imaging planets around BD primaries.

The properties of BDs are so different from those of stars, that two new spectral classes have been proposed for them. The L class is cooler than M. It is characterized by the decrease in TiO and VO bands due to metal condensation in dust grains, and the presence of strong resonance lines of alkali elements (Martín et al. 1997b, 1999; Kirkpatrick et al. 1999). The prototype of this class is GD165B (Becklin and Zuckerman 1988). A second spectral class, either T (Kirkpatrick et al. 1999) or H (Martín et al., 1999) has been proposed for even cooler dwarfs. This class is characterized by the presence of strong methane bands in the near-infrared spectrum. The benchmark of this class is Gl229B (Oppenheimer et al. 1995).

The study of brown dwarfs to determine the multiplicity and mass function is obviously a difficult one, compounded by the relative faintness of the companions and proximity to their primaries. This project will require all of the capabilities of NICI. The low luminosity of brown dwarfs will clearly require the eight-meter telescope of Gemini, as well as the adaptive optics capabilities of NICI, in order to detect these faint objects. The high dynamic range will require the optimized coronagraph and the proximity of low mass companions to their primaries will require the high resolution imaging. NICI's dual channel capability will be an effective tool to identify brown dwarfs spectrally. As discussed above, the lowest mass brown dwarfs have spectral features not found in other stars and sub stellar objects.

Simultaneous imaging in and out of a low mass companion-specific filter, which takes advantage of the spectral signature of these lowest mass objects, will cause these methane-rich objects to stand out sharply in contrasted, subtracted images. We image the field in both broadband and narrow-band filters. Objects that absorb methane, for example, appear in only the broadband image. Thus, the subtracted image will show only the coolest objects, since objects without methane in their atmospheres will appear in both filter images, and thus subtract out. Only the cool low mass companions will remain in the image.

NICI will be able to carry out a deep companion search to a delta magnitude of at least 14 within 0.5 arcsec, thus revealing sub stellar companions (which might typically have delta magnitudes of 5-15 at K band (Burrows et al. 1997)). NICI, optimized for AO and with the added benefit of a customized coronagraph, should be an ideal instrument

for advances in the fields of sub stellar companions and multiplicity. Critical data needed to help constrain the slope of the IMF as well as the multiplicity function below ~0.3 Msun can come from studies of faint stellar and sub stellar companions. With NICI, we will be able to detect companion objects in the range 0.01-0.1 Msun. Brown Dwarfs

2.6. The Search for Extra solar Planets

The direct imaging of extra solar planets is, in many ways, the defining circumstellar imaging problem. There have been many suggestions and claims as to how it should be done, with what instrumentation, at what wavelength etc. The one area of general agreement, however, is that it is very difficult. The problem is, in fact, an extremely complex one that involves both optical imaging properties of the telescope and the physical properties of the planets themselves. We draw on both to present the basic detection considerations. The factors involved in this kind of detection are discussed in some detail because they capture the essence of coronagraphic observing, and illustrate much of the thinking that went into the design of the instrument.

In general, planetary spectra are determined by the reflected light from the stellar primary, as modified by the planetary atmosphere and thermal emission from the cooler planet. Which component dominates obviously depends on the planet, the primary, and the wavelength of observation. Searching in reflected light, one looks for the brightest stars to get the most photons. In thermal emission, we look for the lowest luminosity primaries to minimize the contrast between the star and the planet. We will look, therefore, at planet detection in two contexts: a search in reflected light of the brightest, closest, normal stellar population, and a search in thermal emission for planets around the lowest luminosity objects, particularly brown dwarfs.

Throughout most of the visible spectral region, the spectra of Jovian planets are close to those of the stars they orbit, with some relatively narrow absorption lines arising from the planetary atmosphere. Starting short ward of the near infrared, the reflection spectrum is modified by the planetary molecular composition, with broad absorption features due primarily to methane, and by the increasing thermal emission from the planet. In Figure 2-3 we show some of the evolutionary models for planetary flux density for $5M_J$ planet. The models show that for the thermal component, spectral emission in the near infrared can vary by orders of magnitude with the age and the mass of the planet. Even for normal stars, it is possible in younger systems for the thermal emission to be comparable to the reflected light in the near infrared. In general, the thermal emission peaks for younger and for more massive planets. The latter is important because planet non-detections in thermal emission must be considered as constraints in the age-mass plane.

Through the mid-infrared, the intrinsic thermal emission of the planet generally dominates. This more favorable star-to-planet balance near ten microns has led many researchers to conclude that this is the optimal planet detection wavelength. However there are many more wavelength dependent factors that must be taken into account. The image area over which we collect background increases like λ^2 but the image Strehl

factor also increases like $s_1 \frac{1}{\lambda^2}$ where s_1 is the Strehl factor at a wavelength of 1μm and λ is the wavelength in microns.

The background against which the planet must be detected is the sum of the residual stellar scattered light and the combined sky and telescope background. These background sources must be combined in order to estimate the quantum noise in the detection. Shot noise estimates do not really characterize the difficulty of making this observation because they ignore the systematic aspects of removing the large background in order to get to the quantum noise limit (Brown and Burrows, 1987, Ftaclas, 1992, 1995, Walker et al. 1994). Shot noise estimates give minimum integration times, but it is possible to do considerably worse. Furthermore, no matter how long the estimated integration time is, one could, in principle, just integrate that long. But if the background cannot be removed, the observation cannot be made at all. Experience has shown that the ability to make this subtraction is not at all dependent on the shot noise in the image as long as quantum considerations are satisfied. Handling of the background has been the focus of planet detection for some time.

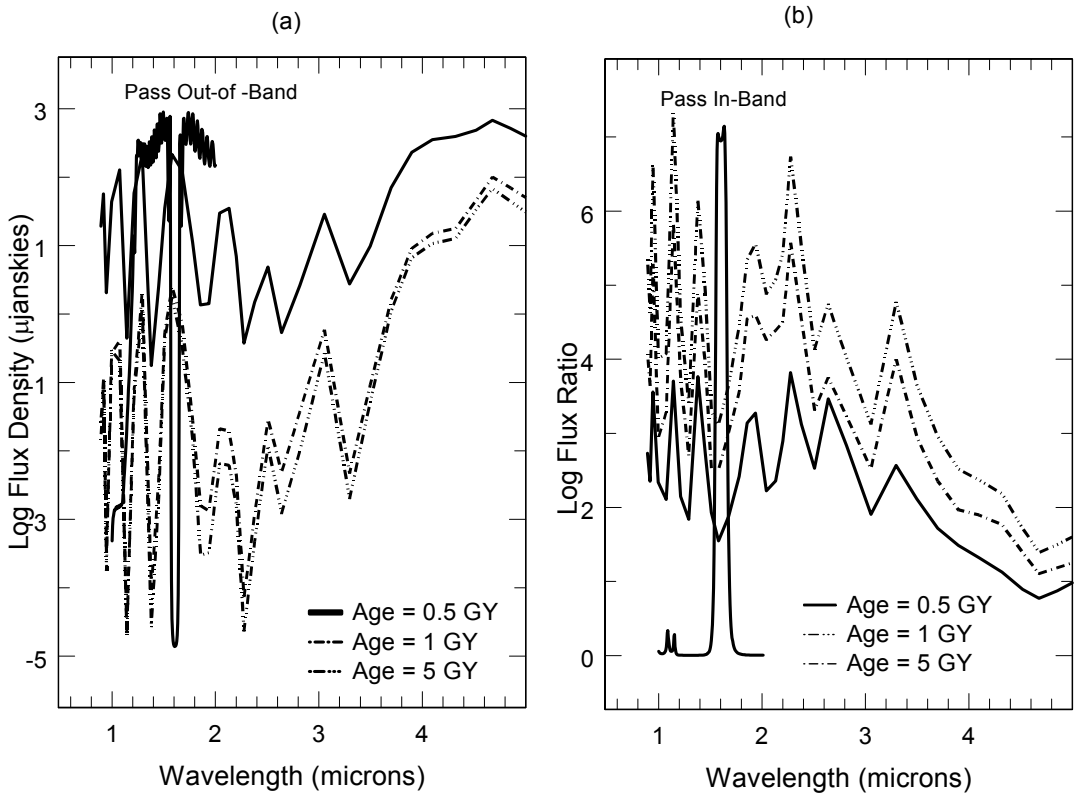

Figure 2-3 (a) Evolutionary models for a 5 M_J Planet and (b) The ratio of the flux ratio for a 50 M_J brown dwarf to that of the planet at the same age. In both plots we have added complementary filter designs meant to isolate the 1.6 micron methane feature.

The sky/telescope background is essentially independent of short-term fluctuations in the seeing record, and can be accurately estimated with frequent beamswitching with small re-pointings of the telescope. The residual scattered light, however, is critically dependent on the detailed turbulence record, and the large pointing changes usually required to find a star of comparable brightness limit repeatability (Terrile 1995, Kalas and Jewett 1996). This occurs even in space observations. Krist et al. (1998) report that in working with NIC images in a search for faint companions, the best they could do with frame differencing was a background reduction to one part in fifteen, and only outside a radius 1.75 arc seconds. Inside this radius, the residuals were significantly larger.

For the Gemini telescopes, the wings of the stellar PSF within a few arc seconds of the star are dominated by the effects of atmospheric turbulence. On average, the scattered intensity will be given by $I_s(\lambda) \propto \frac{1}{\lambda^4} PSD\left(\frac{\theta}{\lambda}\right)$ where $PSD(f)$ is the turbulent power spectrum at spatial frequency f, and θ is the field angle in the focal plane. Again, the leading, strong wavelength dependence has always suggested working at longer wavelengths where the scatter seeks to be lower. The Kolmogorov power spectrum is of the form $PSD(f) \propto f^{-\frac{11}{3}}$ (note that the wavelength dependence of the Fried length is already included in the factor of λ^{-4}). When $f = \frac{\theta}{\lambda}$ is substituted, we get $I_s(\lambda) \propto \lambda^{-\frac{1}{3}}$. Since the scattered light must be collected over the planet Airy disk whose area increases like λ^2, it follows that the scattered light collected per Airy disk will scale like $\lambda^{\frac{5}{3}}$. In other words, as far as scattered light is concerned, the steep atmospheric power spectrum and growing Airy disk size erode the advantage to going to longer wavelengths. This remains true until a significant improvement in the relative brightness of the planet occurs in the thermal infrared. One must also deal with the steep increase in sky and telescope thermal emission at longer wavelengths. For ground-based, scatter dominated imaging of a solar twin system at 5pc, typical values for the ratio of planet peak surface brightness to local background surface brightness are of order 10^{-3} – 10^{-4} in reflected light at 1-2 microns and, of course, can get significantly worse as the apparent angle between the star and the planet decrease. Since the scattered intensity is falling off like $\theta^{-\frac{11}{3}}$, but the reflected light intensity is only falling off like θ^{-2}, it follows that direct imaging is more sensitive to planets at larger orbital radii.

Assuming a planet orbital radius sufficiently large that thermal input from the star is not an issue, then as the stellar luminosity drops, the reflected light component decreases but the thermal emission remains constant. Therefore, the contrast ratio between the star and the planet grows more favorable for intrinsically fainter stars even without going to the mid infrared. The natural conclusion of this argument is to look for planets around brown dwarfs. In the discussions of Section 2.5, we note that the expectation is that by the time NICI is in service, a significant population of nearby BDs

will be identified, so we consider planet detection by thermal emission. There are several compelling scientific drivers for this search apart from those that motivate any planet search. Any companion to a BD is intrinsically of interest, and searching for planets is a natural extension of a faint companion search aimed at determining multiplicity in the BD population. Second, detection of any planet around a BD would determine the mass of the BD, and possibly its age.

In Figure 2-3 we have plotted the ratio of the spectral flux from a 5 M_J planet to that from a 50 M_J BD, again using the models of Burrows et al. Looking only at the minima in these plots (the best places to look for planets) we note that the flux ratio varies only from about 10^2 - 10^5. This is a significant improvement over the value of 10^9, the canonical value for Jovian planets seen in reflected light, and it is achieved in the near infrared. From a background removal point of view, this would be a relatively easy observation for NICI. The difficulty lies in the absolute flux levels. One μJansky is a flux of order $750/\lambda_\mu$ photons s^{-1} μm^{-1} received by the Gemini collecting area (λ_μ is the wavelength in microns). At 1.6 μm this gives a count rate of 470 photons s^{-1} μm^{-1}. The estimated background count at that wavelength is 1.6×10^6 photons s^{-1} μm^{-1} $arcsec^2$. Because of the AO system, the image core at that wavelength is only about 0.04 arcsec wide (FWHM) or just over two NICI pixels wide. The total background count in four NICI pixels would then be 2000 photons s^{-1} μm^{-1} or four times the image counts. Not all the photons collected from the planet end up in the image core, but even allowing for only ten percent in the core, the observation does not look unreasonable. The problem, of course, is that for background dominated observations, the integration time scales inversely with the square of the planet flux. Going down to flux densities of 0.1 to 0.01 μJy, more typical of older or less massive planets, the integration times can get quite long. This case nicely illustrates the value of adaptive optics in background-limited observations, and it is the key to making observations like this.

One important aspect of looking for any companions to BDs is that the ages of all components of the system are constrained to be identical. This is not usually a consideration for reflected light searches, but it is a significant factor for BDs. For example in Figure 2-3the flux ratio at 1.6 μm is about one order of magnitude better than it is at 2μm for an evolved system at 5GY. But it is two orders of magnitude better for the system at an age of 1GY. By determining the flux ratio in different bandpasses, it should be possible, in combination with the evolutionary models, to place bounds on the system age.

Faint objects like brown dwarfs are usually thought of as the object of coronagraphic searches, as opposed to coronagraphic targets. All unresolved sources, however, produce an identical PSF with extended wings. It is more obvious in bright sources, but still there in fainter ones. For BD observations, it is likely that the combined sky and telescope backgrounds will dominate the stellar PSF wings, so NICI will, in all likelihood, not improve the integration time for these observations as it does for bright stars. Once the sky and telescope contributions are removed by beamswitching, however, we are left with an image dominated by the sidelobes of the BD and NICI will reduce that. It is useful to recall that the BD, planet, and background light all go through the telescope as independent (i.e. incoherent), simultaneous experiments.

There are two basic approaches to detecting a planet in a background-dominated image: differencing and filtering. In the former, the image is compared to a reference image in which the planet is not presumed to be present. In the latter, the planet image is detected because it differs in spatial characteristics from its surroundings. If the background were extremely smooth, for example, it would be easy to pick out the steep sides of the planet image core digitally, as long as shot noise considerations allowed it to be detected. An example of this kind of filter (Ftaclas et al. 1994) is shown in Figure 2-4. It depends on the fact that that the effect of bandwidth is to smear speckles radially. The scatter sidelobes are sampled along a radius on either side of the pixel location. These samples are used to generate an estimate of the background at the pixel location, which is then subtracted out, as in high pass filtering. A gap the size of the image core at the pixel prevents contamination of the estimate by the planet signal.

The level of the post-filtered background depends critically on the spatial quality of the input background. For the case illustrated, the rms residual was about ½% of the input. The input was a broadband fixed speckle pattern, so there was no temporal smoothing. One important conclusion from this study was that the post-filter noise level was found to be roughly proportional to the pre-filter input. When noise scales with the background rather than the root of the background, longer integration does not improve the signal to noise ratio. This underscores the assertion that it is background removal that drives the observation, not shot noise.

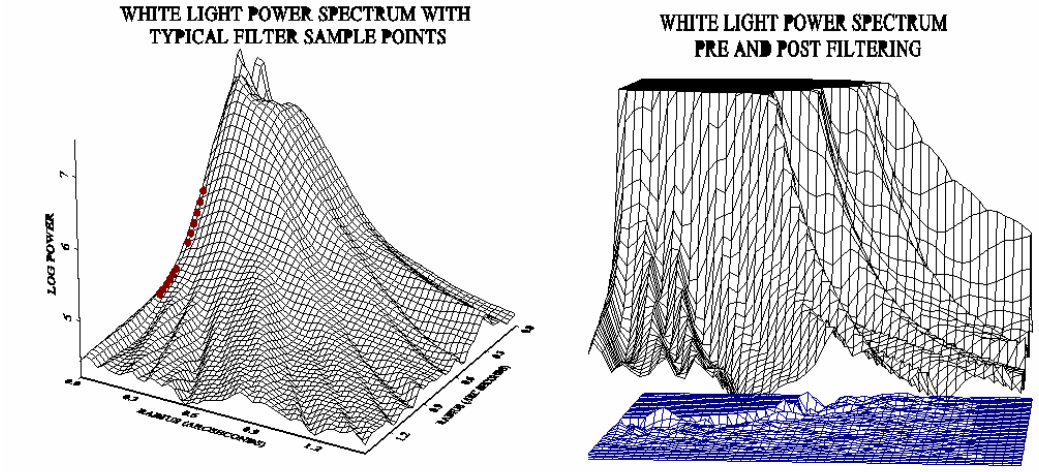

Figure 2-4 A digital filter designed to look for point sources. The log scaled background and sample points are shown on the left. The background (linear scale) and post-filtered residuals are shown on the right.

As noted above, frame differencing has not been particularly effective because of the need to use two different stars. Frame differencing to better than 1% (Trilling and Brown, 1998) is being done at the IRTF using CoCo by imaging in and out of the methane band near K. This approach is very effective because the telescope never moves

off the star, and because the switching can be done relatively quickly to track changes in seeing. Combining these very promising results at the IRTF with the argument that atmospheric turbulence does not repeat (Racine et al. 1999), has led us to consider a dual beam configuration. The goal is to make differential measurements rather than be forced into making absolute comparisons of measurements made hours or days apart.

2.7. Science in Support of NASA Missions

In addition to its charter mission to investigate the birth and evolution of stars and planetary systems, NICI will play a major role in support of other NASA initiatives. As with the IRTF, Keck, and other NASA support facilities, valuable preparatory, follow-up and interpretive work can be done with coronagraphic imaging.

2.7.1 Coronagraphs and Astrometry: (SIM)

There has always been a close connection between coronagraphs and astrometry. Figure 2-5 is an image of Procyon made at the IRTF with the CoCo coronagraphic relay. It was one of the very first images ever taken with the instrument, and was part of a program to image known binaries with large magnitude differences. It turned out to be the first time Procyon and its white dwarf companion had ever been imaged simultaneously. A careful measurement of their angular separation resulted in a new orbit for the pair, and consequently a new mass determination for Procyon (Girard et al. 2000).

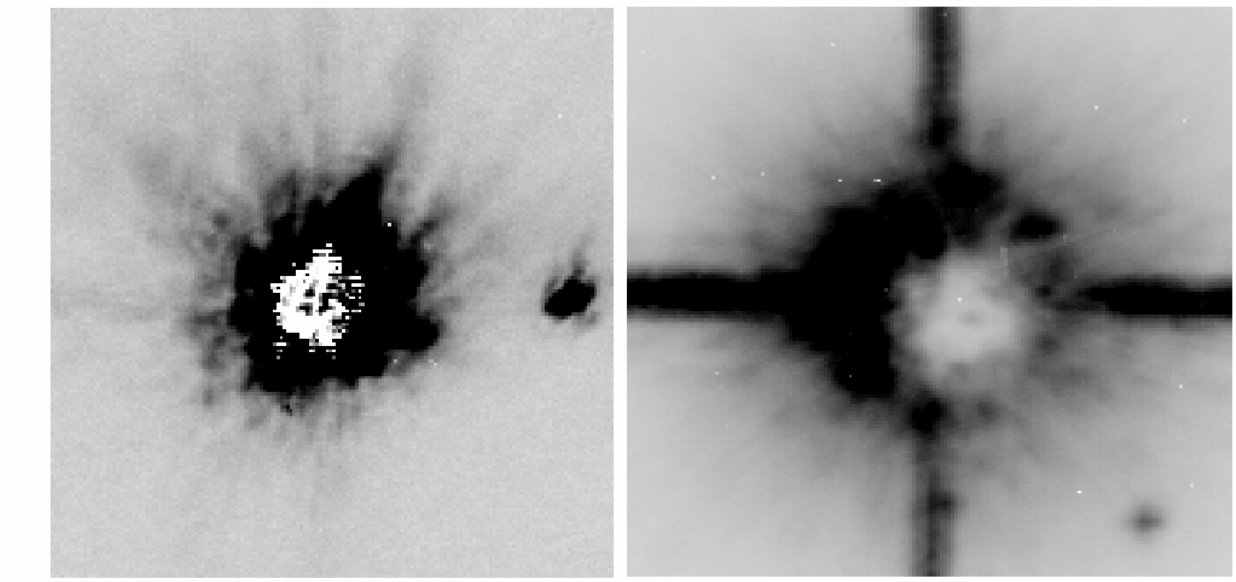

Figure 2-5 Images of Procyon taken at the IRTF with (right) and without (left) CoCo. The white dwarf Procyon b is visible in the lower right hand corner of the right and not visible on the left. Spot at right in left image is a ghost.

When a faint companion is detected for relatively nearby stars, the next step would be a follow-up image separated in time. This serves the two-fold purpose of

verifying the common distance by common proper motion and the beginning of the determination of the orbit. Thus, starting with the image, we move to astrometry for verification and analysis. This relation is purely symmetric. Astrometric observations utilize circumstellar imaging for verification and analysis.

The Space Interferometry Mission (SIM) will be launched in 2006 with a goal of producing high accuracy (4 microarcsec) astrometric measurements on stars as faint as 20th visual magnitude with eight-hour integrations. Depending on the beam combination geometries implemented, it could have some imaging capability, and perhaps a nulling capability for reducing the brightness of a central star to investigate its surroundings. Its goal astrometric precision will be reached over its five-year mission by virtue of repeated measurements made against an astrometric reference grid known to one microarcsec accuracy.

SIM has a rich and varied science program, but the dominant themes are critical distance scale measurements and the search for low mass companions down to Earth-mass objects. There are several symbiotic connections between NICI and SIM. The nature of the grid stars is crucial to SIM performance since there is no other astrometric catalog at that level of precision. Since SIM only measures the centroid of the received light from a star, it interprets all shifts in this centroid as motion of the star. Complex stellar environments can easily produce significant centroid shifts without any real motion of the star. NICI can provide deep imaging of the circumstellar environments of grid stars. It can help evaluate candidate grid stars prior to launch and help resolve anomalies after launch.

Astrometric signals from nearby stars indicating the possibility of low mass companions can be followed up on the ground with NICI. The time scale of the SIM mission is comparable to the periods of inner Solar System planets, but shorter than outer planet orbital periods. Thus, SIM will detect suggestions of long-term, non-linear drifts (as did Hiparcos), but not be able to get complete orbital solutions. With NICI's greater sensitivity to outer planets, it would be possible for a fairly complete search and definition of the closest systems.

2.7.2 Future IR Imaging Missions SIRTF, SOFIA, NGST

After decades of discussion within the community on an infrared capability in space, it appears that NASA has embarked on an ambitious program to create a suite of IR instruments with powerful capabilities. SOFIA, SIRTF and NGST are in various stages of planning, but are all scheduled to come on line in the time frame NICI will be operating. In Table 2-1, we summarize each of these missions with comparable data for NICI. We outline each of these programs below:

The **Stratospheric Observatory for Infrared Astronomy (SOFIA)** will replace the aging Kuiper Airborne Observatory with a 2.5m aperture telescope mounted in a converted jet transport. It will fly over a larger fraction of the water vapor in the Earth's atmosphere than ground-based installations, and image in regions of the spectrum closed to ground-based facilities. Although it escapes much of the atmospheric water vapor, it is subject to enhanced turbulence due to the motion of the plane.

The **Space Infrared Telescope Facility (SIRTF)** will be an 84cm aperture, cryogenically cooled, all Beryllium telescope capable of diffraction limited imaging into the far infrared. It will be in an orbit about the Sun, trailing further away from the Earth as time goes on. Its mission is limited to 2.5 years (with a goal of 5 years) by the lifetime of its liquid Helium supply. SIRTF is designed around its long wave sensitivity and diffraction limited capability. The telescope is not expected to be diffraction limited below six microns

The **Next Generation Space Telescope (NGST),** scheduled for launch in 2009, is currently under aggressive study. It will be a passively cooled, eight-meter aperture telescope in orbit at L2 that will utilize many innovative telescope technologies to control cost and weight. It represents a significant IR capability in space, but in order to deliver an aperture that large to orbit, it will have a segmented aperture and self-erect on-orbit. Segmentation produces a pupil function that is considerably more complex than Gemini's and less favorable for coronagraphic work. The current baseline instrument suite projected for NGST is primarily oriented towards wide-field imaging and spectroscopic modes. Although free of absorption due to the Earth's atmosphere, it is not free of phase perturbations due to its segmented aperture and ultra-lightweight optics, so it is not expected be diffraction limited shortward of 2 microns.

NGST will be able to image in windows where the atmosphere is opaque with a comparable aperture to Gemini, but NICI will still provide valuable services to the project. NICI is a perfect high-resolution follow-up instrument to complement NGST's survey capability. More importantly, as we have indicated throughout this proposal, the defining line between what can be accomplished on the ground and what needs to be done in space has grown steadily less clear. With the very high cost factors associated with almost any space operations, state-of-the-art instruments like NICI will be well positioned to answer significant questions about ground-based near IR imaging, and to provide valuable guidance for final instrumentation, configuration, and tolerancing decisions for NGST.

	SIRTF	SOFIA	NGST	Gemini/NICI
Aperture	0.9m	3.0m	8m	8m
Operating Wavelength	3 -180μm	0.3–600μm	0.6 - 30μm	1-5μm
Diffraction limited wavelength	6.5μm	1 – 5μm	2.0μm	1μm
Minimum Pixel Scale	1.2"	0.12"	0.029"	0.018"
Projected Date of Service	Dec. 2001	Fall, 2002	2009	2004
Platform Type	Solar Trailing Orbit	Air-borne	Space, L2	Ground

Table 2-1 NASA Infrared Capability Over the Next Decade

Looking at the entries Table 2-1, we can see that the total capability is significant and that there are both common areas and significant differences in these facilities. It is easy to imagine a fertile interchange between all of these facilities. We would expect that not only will NICI support observations made with these facilities, it will also benefit from them. Clearly there is a follow-up role for NICI, just as ground based imaging was used to follow up the IRAS detection of excess emission from Beta Pictoris. In this group of instruments, NICI's role of high-resolution deep circumstellar imaging appears to be unique and valuable.

2.7.3 Future Planet Searches

The great difficulty of imaging a planet of any variety has led to a near term focus on Jovian planets because of their larger size and assumed larger angular separations compared to Terrestrial planets. The ultimate goal of the Origins program, however, is the detection and characterization of earth-like planets. To implement this plan, NASA has begun study of a large-scale, interferometric array, the Terrestrial Planet Finder (TPF). The objective is to use a nulling configuration to eliminate the light of the central star, and rotational modulation of the interferometer's fringe pattern to detect planets. Working in the 5 to 10 micron region, it will have a coarse spectral capability with enough spectral resolution to detect the broad spectral features associated with methane, water, Carbon Dioxide and Oxygen. Simulations of the system show that for nearby stars, Earthlike planets could be detected in hours to days, and characterized in tens of days.

The gain of a more favorable star-to-planet ratio at ten microns, however, brings with it some troubling complications for detection. There is the background signal created by the zodiacal emission of our own solar system. This can be overcome by a combination of large apertures and spacecraft orbits close to that of Jupiter. A much less well-understood concern, however, is the effect of a zodiacal cloud in the solar system under observation. Optically, such a cloud would be unresolved in the sub-aperture of the interferometer so that, in effect, the total light of the cloud would appear as background to the planet. For the case of the solar system, that implies a signal from the dust 10^4 times brighter than the signal from the Earth. Moreover, the motion of planets through the zodiacal dust sweeps out lanes in the dust and results in density enhancements of order 10% leading and trailing the planet.

We have good reason to expect that zodiacal dust clouds, where they exist, would cause a bright and structured background for planet detection. The frequency and expected brightness of expected exozodiacal clouds is only weakly constrained by current observations. Models of planet formation show that in only about half the cases does an asteroid belt form which could provide a source of zodiacal dust. Therefore, it is possible that dust will not be a problem in many cases. Arguments based on other observations, however, have concluded that our zodiacal cloud has atypically low density. Given the scale of the TPF mission, it would be risky to fly it without some understanding of the target population. NICI could set upper limits on zodiacal emission, and by imaging very close to primaries, could develop secondary information as to the extent of planet forming activity.

2.8. References

Adams, F.C., Lada, C.J., & Shu, F.H. 1987, *ApJ* 312, 788.

Augereau, J.C., Lagrange, A.M., Mouillet, D., and Ménard, F. 1999

Aumann, H.H. 1985, *ASP* 97, 885-891.

Aumann, H.H., Probst, R.J. 1991, *ApJ* 368, 264-271.

Basri and Martín 1999, *AJ* 118, 2460.

Becklin, E.E., and Zuckerman, B. 1988, *Nature* 336, 656-658.

Beichman, C.A. 1998, *SPIE* 3350, 719-723.

Bodenheimer, P., Ruzmajkina, T., and Mathieu, R.D. 1993, Protostars and Planets IV, 367-404.

Brown, R.A. and Burrows, C.J. 1987, *Icarus* 87, 484-497.

Burke, B.F. 1992, NASA, Solar System Exploration Division Report.

Burrows, C.J., Stapelfeldt, K.R., Watson, A.M. et al. 1996, *ApJ* 473, 437.

Burrows, A., Marley, M., Hubbard, W.B., Lunine, J.I., Guillot, T., Saumon, D., Freedman, R., Sudarsky, D., Sharp, C. 1997, *ApJ* 491, 856.

Chabrier, G. et al. 2000, *ApJ*, submitted.

Close, L.M., Roddier F., Northcott, M., Roddier, C. & Graves, J.E. 1997, *ApJ* 478, 766.

Dermott, S.F., Grogan, K., Holmes, E.K., and Wyatt, M.C. 1998, Exozodiacal Dust Workshop, 59.

Duquennoy & Mayor 1991, *A&A* 248, 485.

Elachi, C. et al. 1996, A Road Map for the Exploration of Neighboring Planetary Systems, JPL Technical Report.

Fajardo-Acosta, S.B., Telesco, C.M., and Knacke, R.F. 1993, *ApJ*, in press.

Fajardo-Acosta, S.B., Telasco, C.M., and Knacke, R.F. 1998, *AJ* 115, 2101-2121.

Ftaclas, C., et al. 1992, HDOS Project –Final Report, PRB110348.

Ftaclas, C. 1995, Proceedings of the Fifteenth National Solar Observatory/Sacramento Peak Summer Workshop, ed. Kuhn, J.R. and Penn, M.J., 1987, (World Scientific, Singapore) 181.

Girard 2000, *AJ*, in press.

Hartmann et al. 1993, Protostars and Protoplanets III.

Jayawardhana, R., Fisher, S., Hartmann, L, Telesco, C., Pina, R., and Fazio, G. 1998, *ApJ* 503, L79.

Kalas, P. and Jewitt, D. 1996, *Astronomical Journal* 111, 1347.

Kastner, J.H., Zuckerman, B., Weitraub, D.A. and Forveille, T. 1997, *Science* 277, 67.

KenKnight, C.E. 1977, *Icarus* 30, 422.

Kirkpatrick, D. et al. 1999, *ApJ* 519, 834.

Knacke, R.F., Fajardo-Acosta S.B., Telesco, C.M., Hackwell, J.A., Lynch, D.K., and Russell, R.W. 1993, *ApJ* 418, 440K.

Koerner, D.W., Ressler, M.E., Werner, M.W., and Backman, D.E. 1998, *ApJ* 503, L83

Koerner, D.W., Kirkpatrick, D., McElwain, M.W., and Bonaventura, N. 1999, *ApJ* 526, L25-L28.

Krist, J.E., Golimowski, D.A., Schroeder, D.J., and Henry, T.J. 1998, *Publications of the Astronomical Society of the Pacific* 110, 1046-1058.

Levy and Lunine, eds., Univ. of Arizona Press, Tucson.

Mannings et al. eds., Univ. Arizona Press, Tucson.

Marcy, G.W., Cochran, W.D., and Mayor, M. 2000, Protostars & Planets IV, ed. V. Mannings, A.P. Boss & S.S. Russell (Tucson: University of Arizona Press), in press.

Marois, C, Doyon, R., Racine, and Nadeau, D., 2000, *PASP* 112, 91.

Martín, E.L., Zapatero Osorio, M. R., & Rebolo, R. 1997a, ``Brown Dwarfs and Extra solar Planets", ASP Conf. Series 134, p. 507.

Martín, E.L. et al. 1997b, *A&A* 327, L29-L32.

Martín et al. 1998, *ApJ* 509, L113-L116.

Martín, E.L., Basri, G., Brandner W. 1999a, *Science* 283, 1718.

Martín, E.L. et al. 1999b, *AJ* 118, 2466.

Martín, E.L. et al. 2000, *ApJ* 529, L37-L40.

Meyer et al. 2000, Protostars and Planets IV, ed. V. Mannings, A.P. Boss & S.S. Russell (Tucson: University of Arizona Press), in press.

Nakajima, T. et al. 1995, *Nature* **378**, 463.

O'dell et al. 1993, *ApJ* **410**, 696.

Oppenheimer, B. et al. 1995, *Science* **270**, 1478.

Oppenheimer et al. 2000, in Protostars and Planets IV, ed. V. Mannings, A.P. Boss & S.S.

Russell (Tucson: University of Arizona Press), in press.

Padgett, D.L., Brandner, W., Stapelfeldt, K.R., Strom, S.E., Terebey, S. and Koerner, D. 1999, AJ 117, 1490.

Racine, R., Walker, G.A.H., Nadeau, D., and Doyon, R. and Marois,C 1999, PASP 111, 587.

Rebolo, R., Zapatero Osorio, M. R. and Marti n, E. L. 1995, Nature 377, 129.

Rebolo, R., Zapatero Osorio, M. R. and Marti n, E. L. 1995, Nature 377, 129.

Reid et al. 1999, ApJ 521, 613.

Scalo, J.M. 1986, Fundamentals of Cosmic Physics 11, 1-278.

Scalo, J.M. 1988, Molecular Clouds/Milky-Way & External Galaxies, 201.

Schneider, G., Smith, B.A., Becklin, E.E., and Koerner, D. 1999, ApJ 513L, 127S.

Smith and Terrile 1984, Science 226, 1421.

Spitzer, L. Jr. 1978, American Scientist 66, 426.

Terrile, R.J. 1995, Private communication.

Trilling, D.E., and Brown, R.H. 1998, Nature 395, 775-777.

Trilling et al. 2000, ApJ, in press.

Walker, G. A., Walker, H., Walker, A., Racine, R., Fletcher, J.M., and Mclure, R.D. 1994, PASP 106, 356

Wang, S., Toomey, D.W., Brown, R.H., Cavedoni, C.P.,. Hua,, R., Stahlberger, W.E., Owensby, P. and Ftaclas, C. 1994, SPIE 2198, 578 (1994).

Weinberger, A.J., Becklin, E.E., Schneider, G., Smith, B.A., Lowrance, P.J., Silverstone, M.D., Zuckerman, B., and Terrile, R.J. 1999, ApJ 525, L53-L56.

Zapatero-Osorio, M. R. et al. 1999, ApJ 524, L115.

3. Science Derived Requirements

By studying the science goals described in the previous sections and references a set of requirements can be distilled that defines NICI. These requirements are called the Science Derived Requirements. The following sections will discuss these derived requirements and relate them to the science discussion concluding with a summary of the combined Science Derived requirements.

3.1 YSOs

The focus for YSO study was high resolution imaging with and without coronagraphic masks. Broadband photometry is required for luminosity and temperature measurements. Coronagraphic masks will be important for some studies although observations very close to the central object will preclude their use at times. There will be shocked gases so differential imaging in and out of ionization lines is required. Filters for on and off [FeII] (1.64 microns) and H_2 (2.12 microns) should be included as well as continuum filters. Light reflected off dust will be polarized so a differential polarization imaging mode is needed. Wavelengths of 3-5 microns are particularly interesting due to penetration of dust and a lack of data at these wavelengths. Beamsplitters with the transition between H - K, K - L, and L – M would be useful for non-differential photometry.

YSO Science Derived Requirements

Requirement	Science Driver
High resolution imaging	Highly structured environment
Broadband Photometry	Luminosity and Temperature
Coronagraphic imaging	Structure in the stellar halo
Non-coronagraphic imaging	Imaging very close to YSO
Emission line differential imaging	Shocked [FeII] and H_2
Polarization differential imaging	Light reflected off of dust
3-5 micron high resolution imaging	Dust penetration, cool objects

3.2 Circumstellar Disks

Since disks are very hard to see coronagraphic imaging is central to the study of Circumstellar Disks(CD) and will require coronagraphic imaging at high resolution using

broadband filters. Since geometries for pole on disks are very favorable for polarization geometries, differential polarization imaging is an important mode. Disks do not have exploitable spectral features for differential imaging making the polarization mode more important for disk studies. Looking for structure in the disk as evidence of planets requires high contrast and good imaging performance on extended objects. Wavelength coverage at short and long wavelengths is desired due to the range of particle sizes and temperatures of the disks.

Circumstellar Disk Science Derived Requirements

Requirement	Science Driver
Coronagraphic imaging	Faint disk, bright central object
High resolution imaging on extended object	To look for structure in the disk
Polarization Differential Imaging	Only exploitable difference feature
1-5 micron wavelength coverage	To probe grain sizes and temperatures

3.3 Brown Dwarfs

Brown Dwarf observations will involve detection and characterization projects. The key detection mode for T Dwarfs will be Methane differential imaging. Warmer dwarfs will be searched for using broadband coronagraphic imaging. Methane features in the H, K and L windows will be important. Observations at M will be used for searches around free floating brown dwarfs. Spectroscopy with resolving powers of ~100-1000 will be used to classify detected companions. High Strehl images are required to aid detection. Astrometry of detected companions is important. Close in imaging will be used to detect radial velocity detected companions. Greater than Nyquist sampling is required.

Brown Dwarf Science Derived Requirements

Requirement	Science Driver
Methane Differential Imaging	Detection and age probe
Coronagraphic photometry	Temperature measurement
Wavelength coverage 1-5 microns	Methane features and contrast with primary
Spectroscopy – low to medium resolution	Companion identification and classification
Astrometry	To measure orbit and record position
High Strehl imaging	To aid detection
Close in Coronagraphic imaging	To search for close in companions

Greater than Nyquist sampling	Greater detection sensitivity
Field of view approximately 20 arcseconds	To get 100 AU field at 5 parsec

3.4 Extra-solar Planets

Extra-solar planet searches will involve coronagraphic imaging at short wavelengths for reflected light and long wavelengths for light emitted by the planet. High Strehl images are important to boost the planet signal above the background light. differential imaging in methane will be important and polarization differential imaging could be used to discriminate planets since they are expected to have high levels of polarization. Characterization and classification will require low to medium resolution spectroscopy.

Extra-solar Planet Science Derived Requirements

Requirement	Science Driver
Coronagraphic imaging	Faint planet near bright star
Wavelength range 1-5 microns	For reflected and emitted light detections
High Strehl images	To aid detection
Differential Polarization imaging	Planets will be highly polarized often
Spectroscopy	Characterization and classification

3.5 Other Science Derived Requirements

During the science discussions two other projects emerged that NICI should be well suited to.

When imaging in regions of high source confusion such as O-B associations, globular clusters or dense star formation regions the wings of the point spread function cause difficulties in measuring aspects of individual objects. A apodized pupil mask can be made that will reduce the diffracted portion of the point spread function wings. This reduces cross contamination of sources in these confused targets.

The study of AGN and Quasars both involve the study of faint structured material near an bright, unresolved point source. Ionization line differential imaging as well as broad band coronographic imaging are used.

Other Science Design Requirements

Requirement	Science Driver
Apodized pupil mask option	High source confusion targets
Ionization line differential imaging	Study of AGN environ

3.6 Science Derived Requirements Summary

The table below consolidates the requirements in the previous sections.

NICI Science Derived Requirements

#	Requirement	Science Driver
SDR1	Coronagraphic imaging	Faint planet or disk near bright star
SDR2	Wavelength range 1-5 microns	For reflected and emitted light detections To probe grain sizes and temperatures Methane features and contrast with primary
SDR3	High Strehl images	To improve detection ability
SDR4	Differential Polarization imaging	Planets will be highly polarized Only exploitable difference feature for disks
SDR5	Spectral Differential Imaging	Detection and age probe for brown dwarfs
SDR6	High resolution imaging on extended object	To look for structure in the disk
SDR7	Coronagraphic photometry	Temperature measurement
SDR8	Spectroscopy – low to medium resolution	Companion identification and classification Characterization and classification
SDR9	Astrometry	To measure orbit and record position
SDR10	Close in Coronagraphic imaging	To search for close in companions YSO and Quasar environs
SDR11	Greater than Nyquist sampling	Greater detection sensitivity

SDR12	Apodized pupil mask option	High source confusion targets
SDR13	Apodized pupil mask option	Study of YSO, AGN environ
SDR14	Field of view approximately 20 arcseconds	To get 100 AU field at 5 parsec
SDR15	Dithering	To improve flat fields

3.7 Translating Science Derived Requirements to Instrument Requirements

The Science Derived Requirements are stated primarily in terms of needed observational modes as well as instrument features. In order to specify the instrument these modes and features must be translated to instrumental requirements. In the sections below each Science Requirement will be decomposed into specific instrumental requirements.

3.7.1 SDR1 Coronagraphic imaging

Coronagraphic imaging is the purpose of NICI. It was a project, from the start, that targeted new levels of performance in coronagraphic imaging and science. Coronagraphic performance must be taken as the highest priority in instrumental choices and be considered in every aspect of the instrument.

On the surface a coronagraphic imager differs from a standard imager primarily in two ways. A coronagraphic imager has an occulting mask in the focal plane and a modified Lyot stop. The second important aspect of the coronagraphic imager is that it is designed to have scattered light characteristics that are less than the residual scatter caused by the atmosphere or in the case of NICI the residual scatter uncorrected by the adaptive optics system. Adding a couple of masks to a camera is easy but achieving the scatter criteria is very difficult. The specific ways in which the coronagraphic requirements are listed below:

Low scatter optics- The scatter within the instrument should be less than the residual atmospheric scatter after adaptive optic correction. Optical design should minimize ghosting and minimize the number of surfaces.

Multiple focal plane and pupil plane masks – To optimize coronagraphic performance over a wavelength range of a factor of 5 multiple masks will be required that are real-time selectable. Matching pupil plane masks will also be required.

Pupil Imager – Optics that reimage the pupil after the Lyot stop is required to optimize coronagraphic performance and verify alignment.

Rotating Spider Mask – Unless masked near the lyot stop the diffractive spider flares will be the brightest source in the focal plane. On Gemini the pupil rotates with respect to the focal plane sweeping these bright spider flares across the image. A cross

shaped mask placed near the Lyot stop can substantially reduce these flares but the mask must rotate in coordination with the rotation of the instrument rotator.

Numerous science applications such as disk imaging, cool companions and YSO require images over the 1-5 micron range. An In:Sb detector or one of similar bandpass is required. The Optics must pass wavelengths from 1-5 microns with very little change in magnification with wavelength. Reflective optics would be preferred.

The coronagraphic reduction of image sidelobes is produced by the combined effect of a focal plane occulting mask and a pupil plane Lyot mask. The goal for NICI is to reduce the background to its lowest possible level. The scatter caused by the atmosphere and the telescope, elements external to NICI, defines this floor below which the sidelobes cannot be reduced.

Broadly speaking, the AO system reorganizes energy that started close to the image core into a new higher image core but has little effect further out in the field. Because the atmospheric power spectrum is steeper than that of the telescope we expect atmospheric scatter to dominate over most of NICI's field of view. Thus we take as a requirement for NICI coronagraph design that it is capable of being environmentally limited. That is, no matter how good atmospheric conditions and the telescope finish are, the residual intensity in the focal plane will always be dominated by factors external to NICI. This assures that we have done the best job possible of reducing atmospheric scatter. Because scatter essentially adds in an optical system, NICI's optics cannot help but increase the total scatter level but we want to keep that increase smaller than the two dominant sources the atmosphere and the telescope. We anticipate, based on figure results reported so far for the Gemini optics, that the atmosphere dominates all other scatter sources.

For a given level of coronagraphic reduction, there exists a range of occulting mask and Lyot stop pairs that will produce a scatter limited focal plane. As one increases the occulting mask size, the Lyot stop can be opened up for the same performance. Thus one is trading field of view for throughput, while keeping performance constant. This tradeoff is important to NICI. As we have noted, the instrument must operate over a factor of five in wavelength. Occulting masks are measured in Airy rings implying that if we keep the Lyot stop constant the occulting masks must span a fivefold range of radius in order to maintain the same performance. But we only have three positions for occulting masks and effectively three positions for Lyot stops so we will have to be careful in choosing our elements.

The basic strategy is as follows: We have a low medium and high throughput Lyot stop and a small medium and large occulting mask. We start at the shortest wavelength with the smallest occulting mask and highest throughput Lyot stop and require that it be scatter limited with some margin. As the wavelength increases that margin is used up and we must go to the medium throughput Lyot mask and so on. In this way we can go through the nine possible mask-stop combinations and design them to span the full operating range of the instrument.

3.7.2 SDR2 Wavelength Range 1-5 Microns

High spatial resolution near infrared imaging is intrinsic to the NICI science program. For example, imaging in shocked lines of [FeII] at 1.64 microns and the 1-0 S(1) line of H_2 at 2.12 microns is essential to the YSO study. Observations made with other instruments showed that Methane difference imaging is a very powerful technique for detecting low mass companions, and is expected to be one of the most powerful techniques for this instrument. The question is then how far into the visible and IR should the instrument wavelength capability be extended. Adaptive optics (AO) is crucial to NICI's success, since it permits the small image cores and high encircled energies necessary for the detection of faint objects.

For most observations, the AO guide star will be the object being investigated, and in many cases it will be relatively cool as in the case of YSO's and Brown Dwarfs (BD's). There is thus a conflict for photons between the AO system and the camera at the Vis/Near IR boundary. This is especially true since with AO the smallest images would be achieved at the shortest operating wavelength. However, as there are no strong science drivers near one micron, it would make sense to allow the long wavelength cutoff of the avalanche photo diodes (APDs) of the AO system (0.9 microns) determine the short wavelength cutoff.

The long wavelength cutoff of the instrument is affected by a number of factors. The budget does not allow for multiple detectors, so the need for a single detector for near IR imaging implies either 1.0-2.5 microns with HgCd or 0.8-5.5 microns with InSb or the new long wavelength HgCd. An important discriminator between these possibilities is the relative importance of L and M wavelengths.

The primary instrumental science goals established the importance of looking for massive companions to the growing population of known Brown Dwarfs (BD). Such companions are crucial to the determination of BD masses, and are themselves an interesting population of planet/BD objects. The question is whether to look for these companions in scattered light or self-emission. Analysis of the Burrows et al. structural and evolutionary models of low mass objects showed that the ratio of the spectral emission from a 50 M_j BD to that from a 5 M_j planet was a minimum at five microns almost independent of the age of the system, and was significantly more favorable than the geometric scattered light expectation. This stands to reason since, unlike scattered light, self-emitted light will be most visible next to the faintest parent. The contrast ratio at M can be as many as five orders of magnitude less than it is at K.

Follow up work on Gl229b has shown the value of L photometry in fitting low mass objects to evolutionary models. Understanding cold circumstellar disks benefits significantly from multi wavelength observations with long wavelength observations essential for determining the particle size spectrum and disk temperatures. Without an L and M band capability, important follow-up work to any disk or companion detection would have to be done at other telescopes or not at all, if no other instrument with the sensitivity of the Gemini system exists. Since spectral characterization is an essential part of the Origins and general science agenda, it was considered essential to develop an instrument that could operate over the full InSb band pass.

Additional justifications for the need to include operation to the longest practical limit include the need to image YSO's and the need to characterize the composition of particles in circumstellar disks. In the case of the former, the longer the operating wavelength the earlier in its evolution the protostellar object can be studied. In the case of the latter, the general shape of the particle reflectance spectrum over the 1-5 micron can help distinguish between ice (collisional) and mineral (subliminal) particles. In summary, operation to five microns is clearly mandated by the instrument science goals, even though a limited, pure discovery agenda could conceivably be carried out with just a narrower 1-2.5 micron operating bandwidth.

3.7.3 SDR3 High Strehl images

The requirement for High Strehl images or compact images from an 8 meter telescope means that adaptive optics are required. The challenge is to improve the strehl without creating undesirable scatter effects. The curvature base AO systems produce less scatter from the deformable mirror than the stack actuated mirrors and are preferred for this instrument. The present State of the Art for curvature systems is around 85 elements. On Gemini an 85 element adaptive optics system will produce 80% Strehl ratios at 2.2 microns with guide stars as faint as 14^{th} magnitude. While higher performance could be used at the shorter wavelengths the 85 element provides most of the correction one could ask for while not stretching the present technological limits too far and is chosen for the baseline for NICI.

High Strehl Imaging also requires that the optical elements of NICI must be of very high quality. Very high strehl optics for the science channels and the WFS that produce strehls of at least 80% should be the goal.

3.7.4 SDR4 Differential Polarization imaging

Differential polarization imaging could be implemented in two ways. Fist through the use of a polarizing beamsplitter and second through the use of fixed wiregrid polarizers in each filter wheel. Additionally the instrument should have a minimal instrumental polarization. Optimizing for low instrumental polarization would drive towards a centered, transmissive optical design. The coronagraphic performance issues drive toward a off-axis reflective design. Instruction from Gemini after the conceptual design review was to not pursue the polarization mode and to emphasize the coronagraphic performance. NICI, however will not have an excessive instrumental polarization and should be usable in this mode with a polarizing beamsplitter and it is likely that this mode will be experimented with in the future.

3.7.5 SDR5 Spectral Differential Imaging

This might be called the prime observing mode for NICI when used in the coronagraphic mode. There are a few drivers from this requirement. Foremost NICI must be a dual channel imager and since the images will be differenced the two channels must be as similar as possible and must be referenced to each other. Most often NICI will be used at wavelengths very close together and there are many different wavelengths of interest. NICI is required to have at least 12 dichroic or beamsplitter positions.

Dual Beam Simultaneous Field

The dual beam simultaneous imaging aspect of NICI is central to its power. Probing the speckle noise dominated environment in the stellar halo, differential imaging can be done best by taking simultaneous images. In order to realize the inherent power of dual channel imaging, we impose the following subsystem requirements:

a) Timing - In order to preserve the identity of the two channels in the face of atmospheric turbulence, the two arrays must be clocked such that the two integration intervals are simultaneous to a small fraction of the total integration time. This means that the detectors are triggered to begin integration within some small time interval *dt* and that they each expose for the same time period to within *dt.* We can estimate *dt* by the following argument: Scatter at *N* Airy rings is caused by errors of spatial frequency *N* cycles per aperture or spatial period *P=D/N* where *D* is the telescope aperture. This scatter will change on a timescale comparable to the time the phase pattern takes to move a distance *P.* Thus it scatters at the edge of the field that changes most rapidly and puts the most stringent specifications on event timing. At K band, the edge of the field corresponds to about 200 Airy rings, so the scatter arises phase errors of period 4 cm. At a wind speed of 10 m/sec (36 km per hour) the phase pattern moves by 4 cm in 4 msec. To allow for variations in wind speed and other uncertainties, we take as a working specification an event timing accuracy of 1 msec. This also corresponds to the outer loop frequency of the AO system, so at this level we will not be making timing errors that exceed the AO measurement cycle. One millisecond is also less than 1% of the typical integration times expected over the NICI operating wavelength. We note that, in general, if *dt* is the uncertainty with which we can trigger any event in the instrument, then the rms difference in the duration of any two 'simultaneous" events is *2dt.* So we need to apply the appropriate timing specification to assure our integration intervals are synchronized.

b) Optical Path – In order to maintain the equivalence of the imaging channels, we need to control optical differences between them. These differences can impact the system in several different ways:

   (i) Figure error differences. If the non-common path optics have very different figure their imaging properties will vary. Once the beam passes the Lyot stop, most of the dominant central light has been eliminated so the concern here is not scatter. The issue is the image quality of non-central images that can introduce artificial colors and related effects. The fractional difference in the Strehl factors of the non-common path optics is *2sr* where *s* is the fractional difference in total figure between the two paths and *r* is the fraction of the total figure in the non-common path. Typically *r* can be estimated as the square root of the ratio of the number of elements in the non-common path to the total number of elements in the path. In

this case, however, the dominant sources of figure error are the atmosphere and the telescope itself, so the four non-common path optics are only a small fraction of the total. We take as a working specification that the Strehl ratios in the total path of the two channels differ by less than 1% of their average value and will revise this as more data is received from manufacturers. This figure is exclusive of focus and power, which are treated separately below.

(ii) Focus Differences. Overall focus of the detectors is a relatively soft requirement because of the slow beam, but differential focus error is a more significant problem. First of all, any significant uncorrected differential focus errors would contribute significantly to the Strehl difference between the two channels. Second, focus changes would alter the image structure in the two channels, so that even with a neutral split the two channels would not difference satisfactorily. We are currently developing specifications for the differential focus tolerance and will update this document when this work is completed. We note that because focus degrades the Strehl and increases image sidelobes, it is not removed by any simple processing transformation.

(iii) Power Differences. It is possible we could have identical figure in both channels and have both channels in perfect focus, but the magnification could differ. Simple magnification is, in principle, just an overall scale factor, but in reality trying to overlay one frame with another, one generally encounters plate constants or scaling transformations that are more complex. We want to assure that with a neutral split, our two channels will subtract to within a factor that is better than our current frame differencing work at IRTF, which is in the range 1.0-0.1%. We will develop a standard mapping procedure that will periodically allow for updating the coefficients of a transformation that will map the two channels onto one another. Clearly, the more frames have to be interpolated the larger the corrections being applied and the more our accuracy is degraded. Therefore, it pays to control the power difference in the two channels at the outset. Optics in the two imaging channels will be diamond turned as pairs, with specifications not only of the figure but the figure differences. Working with the manufacturers, we will develop specifications to assure that the channel mapping is as accurate as possible.

(iv) Dichroics. One non-common path element that requires special attention is the beam-dividing element that defines the two channels. We will refer to it as a dichroic, but we understand it

could be a range of possible components, implementing a variety of beam division strategies. This element is partly common path and partly non-common. Of particular concern is that coating stresses could induce a curvature in the element that changes the power of the reflected beam, but leaves the transmitted beam unaffected. We need to make sure the substrates are substantial enough to minimize these effects. We will have several test dichroics made to evaluate these effects and work with coating suppliers to assure that the level of any curvature is acceptable. The dichroics must be mounted so that the angle of reflection is uniform when dichroics are changed

Array Position. The arrays must be mounted so that precision, translation, and rotations can be made to match the two array positions as closely as possible. Even with great care, it is doubtful that the arrays can remain aligned with each other in every mode and at all angles to the desired $1/10^{th}$ of a pixel or 2.7 microns. A position calibration mask will be made that allows calibration images to be taken so that one array can be mapped to the other.

Dichroics, Filters and Channel Splitting Options

There are 24 filter positions in each imaging channel and positions for 15 possible channels separating elements. These components work together to enable a given observing strategy. There are many possible combinations to permit maximum creativity on the part of the observer. We give some typical observing scenarios below:

a. By using a dichroic to split the beams with bandpass filters downstream in each channel filter wheel one can do simultaneous two color filter radiometry. This is an efficient way to classify a large sample of objects and save valuable telescope time.

b. By using a polarizing beamsplitter to divide the channels one can do two-channel polarimetry in identical bandpasses or other more complex combinations.

c. By using a narrow band filter to divide the channels, in-band information is sent to one channel and all out-of-band to the other. Filters in the individual channels can then shape the out-of-band to make the necessary continuum measurements. For a given spectral line it may be advantageous to sample the continuum by straddling the line, or by measuring longward or shortward of the line. Filter choices will be designed to work with line filters to allow several possibilities for continuum measurement.

d. Several methane-differencing strategies are possible based on H, K and L features. These can be implemented in a variety of ways using either a long short dichroic split with downstream filters in each channel or using the line itself to generate the split and measuring the continuum as

described above. We are also investigating making the line splitting filter in a polarized version so one can search not only for methane, but also for polarized methane emission.

The most important function of the two-channel camera is to permit the rejection of residual background. Because we are observing in the immediate vicinity of the AO guide object we have no problems with changes in the isoplanatic patch associated with using two separated stars. Because we are observing simultaneously we have no problem with the repeatability of the atmospheric record. But because we are often observing at two different wavelengths, we have a fundamental focal plane scaling issue associated with the wavelength difference. This raises the issue of the best way to scale the two channels onto each other. Experience with NICI will serve to define some of these approaches and others will be tested while NICI is being designed and built.

For line/continuum observations in particular there are several strategies to making the best continuum measurement. It is impossible to say which is best at this time particularly since it is rare that a spectrum consists of a single line in a flat continuum. Where the spectrum has complex structure it will be necessary to have some flexibility in making the continuum measurement. One consequence of the flexibility inherent In the NICI design there are often two ways to make the same observation. For example instead of using a long/short channel split and bandpass filters in each channel one could use a 50/50 neutral density channel split and the same bandpass filters. The latter is less efficient but it is an important verification tool. Furthermore, in this mode, the role of the two channels can be reversed for further confirmation of a given observation.

3.7.6 SDR6 High resolution imaging on extended objects

High resolution imaging on extended objects shares requirements with high Strehl Imaging . They both require adaptive optics and high quality optics. The extended object imaging has addition requirements, specifically an apodized pupil mask optimized for reduced wings in the psf.

3.7.7 SDR7 Coronagraphic photometry

Coronagraphic Photometry requires that the instrument have standard J,H,K',L' and M' filters.

3.7.8 SDR8 Spectroscopy – low to medium resolution

The spectroscopy option requires the addition of a slit in the focal plane wheel and space in the filter wheels for the grisms. The background levels through the grism will dirve the dark count requirements for the instrument. Spectral information is desirable over the hole 1-5 micron range. Low resolving powers of 100 are used for spectral typing and higher resolutions are used for more detailed studies. Room should be left in each filter wheel for two grisms. One position in the focal plane wheel will be needed for the slit mask that will have two slits of different sizes.

3.7.9 SDR9 Astrometry

Follow up of discovered companions will require tracking positions accurately. Stable positioning of the optics and arrays is important. The distortion each channel must be characterized.

3.7.10 SDR10 Close in Coronagraphic imaging

Close in Coronagraphic imaging requires small focal plane masks and the matching pupil plane masks. A open or no mask mode is required for the focal plane wheel so that speckle observations can be done for very low separation objects. A user position should be provided in the wheel to allow experimentation with phase masks.

3.7.11 SDR11 Greater than Nyquist sampling

For an instrument like NICI to cover an operating wavelength range of more than a factor of five with no change in plate scale, some performance trade-offs must be made. The magnification of the optical will determine the plate scale at the final instrument focus, but choosing that magnification, i.e. pixel size in arc seconds on the sky, necessarily involves a compromise between many performance issues including:

a. Field of view
b. Image processing issues
c. Detection sensitivity
d. Photometry
e. Background levels/Array Readout rates

In the absence of a specific observational scenario with well-defined constraints, there is no "best" or optimal pixel size. We can only try to anticipate the nature of the science observations we have defined, and try for a reasonable compromise based on the performance issues given above. Toward this end, we discuss each of these issues below.

a. Field of View – For the target science objects range from the closest stars, to star forming areas out to 150 parsecs, and beyond. For mature planet or disk systems, we assume that we would like our field of view to encompass a radius of order 100 AU. For star formation processes, we would want to image a radius as large as 1000AU. Fields of view with the following radii would be required for these two cases:

Disc Apparent Radius versus Distance

	5pc	10 pc	20 pc	150pc	1000 pc
100 AU Radius	20 arcsec	10 arcsec	5 arcsec	0.7 arcsec	0.1 arcsec
1000AU Radius				6.7 arcsec	1 arcsec

The driver here is the need to image objects at large field angles for the very closest systems. In terms of target density, there are 10 times as many stars out to 10 pc as there are out to 5 pc, so it makes sense to weight the magnification toward the 10-parsec sample if a tradeoff must be made. The closest objects are attractive since their larger angular separation makes for improved S/N, but, even for a 10-arcsec field radius,

objects in Pluto's orbit could be imaged in systems as close as 4 pc. In summary, the bulk of the core science could be accomplished in a 20-arcsec-radius field, and there would be little loss of science in a field as small as a 10-arcsec radius.

b. Image Processing Considerations. The detection of faint sources requires both instrumental performance and effective postprocessing of the data. We can anticipate the general considerations that enter into typical postprocessing scenarios and consider how they would affect instrument plate scale:

Deconvolution techniques – Experience with the deconvolution of images from Space Telescope suggest a pixel scale of more than three, but less than four pixels per λ / D (D the telescope diameter[1]). The simple answer here is that the sampling needs to be consistent with the final image size after deconvolution, which is typically half the sampling size of the preprocessed image.

Background removal techniques – In searching for point sources, one is aided in background removal by knowing the signature of the object of the search. The major signature difference between a point source and features in the broadband background is the steepness of the sides of the slope of the point spread function (PSF) core. Anything that accentuates this steepness makes a faint point source easier to detect and also drops the false detection rate. Improving image Strehl, for example, steepens the sides of the PSF. Sampling over any finite pixel area, however, always degrades the effective core Strehl since it is essentially an averaging process. Moreover, higher sampling density means more accurate background modeling, which also aids in detection. Three to four pixels per λ / D are minimal for these types of techniques. A higher sampling rate would be desired if it did not diminish field of view or compromise S/N.

Point spread difference techniques – Techniques that involve the differencing of point spread functions from different objects, or at different wavelengths, work relatively poorly at minimal, or Nyquist sampling density. This occurs because at critical sampling density, shifts of a fraction of a pixel cause a very different looking PSF that will not difference well. As in the paragraph above, for PSF differencing, higher sampling densities are called for. Results obtained at the IRTF with .056 arcsec pixels and ~ 0.3 - 0.5 arcsec images have been among the best obtained anywhere without real time chopping. This is 5-9 pixels per image core radius and argues for substantial over-sampling of the image core.

c. Sensitivity – Historically pixel density arguments have centered on achieving maximum signal to noise in a given time for a read noise limited scenario. This argued for large pixels to get enough flux to be background limited, despite a large read noise penalty. Cameras were typically two pixels per λ / D or less. The present generation of

[1] Private communication with Dr. Eric Tollestrup Smithsonian CFA

arrays has much lower read noise, and it is not difficult to achieve background-limited observations in tens of seconds, even with very small pixels. Multiple sampling reads with the Aladdin array achieves read noise levels of around ten electrons. To be background limited at broadband J, it would only be necessary to integrate about ten seconds to collect 200 electrons worth of background with .018 arc second pixels. Most early observations were also made on objects that were as bright or brighter than the background, so that spreading out the image or under-sampling it had little or no consequence other than some modest degradation in the transfer function. Coronagraphic observations, by their very nature, however, seek objects much fainter than the background. In the background dominated imaging regime, spreading out the image, or under-sampling it carries significant penalties. Maximum sensitivity also argues for the smallest possible pixels that don't compromise S/N or field of view.

d. Photometry – Accurate photometry, i.e. <5%, requires proper accounting of all of the flux from a star normalized by the flux from a standard. Array pixels do not have uniform response from pixel edge to pixel edge. Although modern arrays do not have dead space between the pixels, there is a travel distance difference for photons that are detected at the edge of a pixel compared to one at the center, and more time for the electron hole pair to recombine before reaching the diode junction. This results in a falloff of the response at the edge of the pixel. This is very hard to measure since pixels are typically ten times larger than the wavelength. As the angular scale of the pixels increases, a significant fraction of the flux can be lost down these "cracks" in a highly position dependent way. This introduces an uncertainty in the object to standard flux ratio. There is little data presently for the Aladdin array, but based on previous experience, two pixels per λ / D are required to achieve photometric errors below 5%.

e. Background levels/Array Readout Rates – Driving pixel scale to higher values results in a loss of image contrast due to undersampling of the image. But it could also lead to a readout problem if the ambient background fills up the pixels faster than we can read them. The expected background counts for NICI on Gemini South, with a total emissivity of about 6% and a pixel size of .018 arcsec, are given in the table below:

Photons/sec/pixel versus Wavelength

Filter	**J**	**H**	**K**	**L′**	**M′**
Counts	20	45	58	51840	174960

Choosing the largest pixel size that permits full-frame readout at five microns could set pixel size. The Aladdin arrays can presently be read out at about 10-12 Hz frame rate for a double correlated sample. Well depths vary from device to device with a low of around 70,000e to a high of almost 200,000e. This would imply a maximum flux rate of about 700,000 to 2,000,000 e/s/p. This would yield a maximum pixel size of .036 - .064 arcsec to allow readout M.

Choosing Pixel Size

As noted above, the science drives a wavelength range that varies by a factor of five, but the budget permits only a single plate scale if we are not to compromise the fundamental mission of the instrument. In the absence of AO this would have been less of a concern. In this case as the wavelength increases, diffraction increases the image core size, but scattering effects due to the atmosphere decrease and the image core size does not grow linearly with wavelength. In fact, the image core radius actually reaches a minimum near K for typical atmospheric conditions and telescopes few meters in aperture. With a quality AO system, however, we are always assured of an image core diameter proportional to the wavelength, and consequently the effective sampling must necessarily vary by a factor of five.

The decision was made to choose a magnification that gave minimal sampling of two pixels per λ / D at J band so that we did not compromise photometry at J. This gives us 3.5 pixels per L/D at K band, which satisfies most of the imaging considerations discussed above. This magnification gives a .018 arcsec/pixel sampling, assuming an eight-meter telescope with a 90% Lyot stop. The sampling versus wavelength is as shown below:

Sampling versus Wavelength (0.018 arcsec/pixel, 90% Lyot stop)

Band	**J**	**H**	**K**	**L′**	**M′**
Wavelength	1.2μm	1.6μm	2.2μm	3.8μm	4.8μm
Pixels/ λ / D	2.0	2.6	3.5	6.1	7.5

The resulting field of view for a 1024 X 1024 array 9.1 arcsec radius for the largest inscribed circle. A second plate scale might be desirable. However, the core science driving the instrument is intrinsically narrow field, circumstellar imaging. In designing the instrument to fixed cost, all design decisions were made in favor of supporting the core science program as the highest priority.

In summary, the science program requires the detection and characterization of very faint objects. These background-dominated detections involve several techniques that argue for the highest pixel sampling density possible. Limiting the sampling density are practical considerations like finite detector size, field of view requirements, and costs associated with the number of independent plate scales. We have chosen a single pixel scale of 0.18 arcsec/ pixel because:

1. It provides minimum acceptable sampling at J band

2. It gives a 9.1-arcsec-radius field of view that minimally satisfies the field of view requirement derived above.
3. It can be read easily at L and M bands.
4. It is well sampled at K, where much of the science agenda will be carried out.
5. It permits accurate photometry at all operating wavelengths.

Implementing just one plate scale results in significant cost and complexity savings that will be applied to other subsystems (AO, dual channel architecture) that directly impact achieving the core science.

3.7.12 SDR12 Apodized pupil mask option

For high contract imaging and photometry of densely pack areas of confusion an apodized pupil mask is required for the pupil wheel

3.7.13 SDR13 Ionization line differential imaging

Ionization line imaging requires line filters and continuum filters for each line of interest.

3.7.14 SDR14 Field of view approximately 20 arcseconds

Most coronagraphic projects require small fields but nearby objects can get large. The selected field of view of 18 arcseconds diameter is the result of using a 1024 array with the required 0.018 arcsecond per pixel sampling. This represents a balance between sampling and field of view for the 1024 array.

3.7.15 SDR15 Dithering

Dithering requires that the focal plane mask move with respect to the focal plane. One dimensional dither is sufficient since only the number of independent position is important. Dithering also requires that the wavefront sensor boresight must shift with respect to the science array. A steering mirror or equivalent must be included in the wavefront sensor.

3.7.16 Summary of Top Level Instrumental Requirements

The table below summarizes the derived Top Level Instrument Requirements for NICI.

#	Requirement	#	Instrumental Requirement
SDR1	Coronagraphic imaging	IR1 .	Multiple focal plane and pupil plane masks
		IR2	Low scatter reflective optics
		IR3	Low Ghosting optical design
		IR4	Pupil Imager
		IR5	Rotating Spider Mask

SDR2	Wavelength range 1-5 microns	IR6	In:Sb detector
SDR3	High Strehl images	IR7 IR8	High Strehl optics Adaptive Optics
SDR4	Differential Polarization imaging	IR9	Polarizing beamsplitter
SDR5	Spectral Differential Imaging	IR10 . IR11	Many beamsplitters and filters for required modes Dual Channel Camera
SDR6	High resolution imaging on extended object	IR7 IR8	High Strehl optics Adaptive Optics
SDR7	Coronagraphic photometry	IR14 IR15	Broadband filters Many filter locations (>20)
SDR8	Spectroscopy – low to medium resolution	IR16 . IR17	Grism spaces in the filters wheels A slit position in the focal plane wheel
SDR9	Astrometry	IR18 IR19	Stable positioning Characterized distortion
SDR10	Close in Coronagraphic imaging	IR20 IR21	Small focal plane masks A no mask mode
SDR11	Greater than Nyquist sampling	IR22	.018 arecsecond pixels
SDR12	Apodized pupil mask option	IR23 IR24	Apodized pupil mask Room in the pupil mask wheel
SDR13	Ionization line differential imaging	IR25	Filter locations for at least two filters per line
SDR14	Field of view approximately 20 arcseconds	IR26	18 arcsecond diameter field
SDR15	Dithering	IR27 IR28	Moveable focal plane mask Steering mirror in OIWFS

.

4. Instrument Design

4.1. Overview

At its simplest level, a coronagraph can be made by merely adding a field stop and Lyot stop to a camera. Yet no project that has tried this straightforward addition has resulted in a successful instrument. In the solar community, the term "coronagraph" is used to refer to the telescope and instrument combined because in the presence of the overwhelming flux from the solar disk, it is abundantly clear that it is the whole system: site, plus telescope, plus camera, that determines performance. This realization remains valid in the stellar case but it is considerably less obvious and the instrument has come to be considered more an add-on. In the NICI instrument we have the unprecedented opportunity to come closer to the solar ideal than has been heretofore possible.

The Gemini program is creating state-of-the-art telescopes with outstanding image quality at two of the world's premier sites. NICI will sit at the focus of those telescopes and from there to the instrument final focus the design has been optimized to achieve the deepest possible circumstellar imaging. The instrument is unique in that it is the first of its type designed solely for this purpose with none of the performance compromises typical of multi-use instruments. Intrinsic to the design is the enabling quality of the instrument. Its dual channel design and multiple filter wheels and beam division options encourage observer innovation and greatly facilitate background subtraction. Moreover, the multiple filter and stop wheels permit easy modification to accommodate future invention, and future observational problems. A dedicated adaptive optics system will be built in to the instrument. This offers significant simplicity compared to more complex facility systems and assures that the design will minimize scatter while optimizing the concentration of energy in the focal plane. All in all, because the instrument has a single clearly stated goal, it has a deceptively simple design thoroughly optimized to meet that goal.

A block diagram of the NICI instrument is shown in Figure 4-1 and a schematic of the optical train is shown in Figure 4-2 .

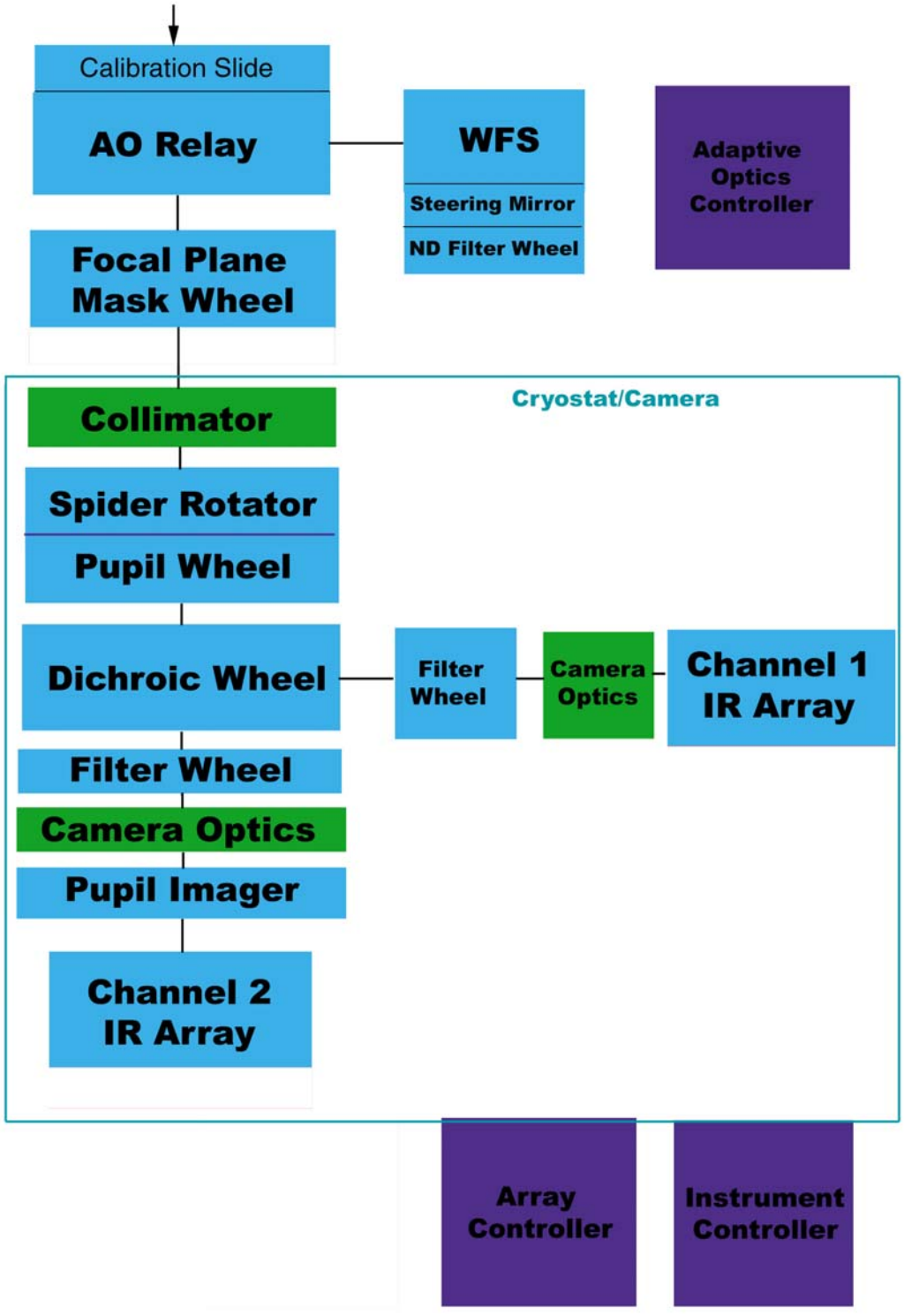

Figure 4-1 Block Diagram of the NICI Instrument.

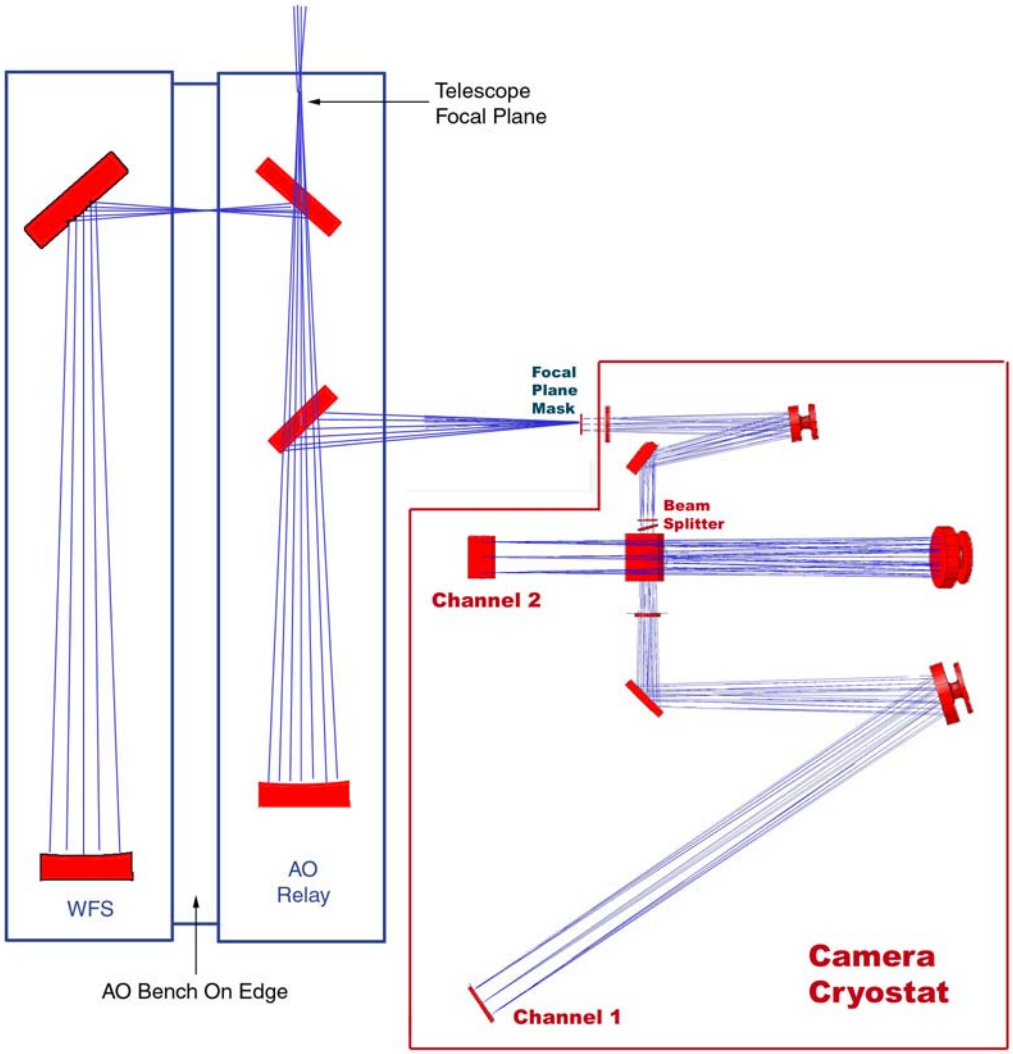

Figure 4-2 Optical Schematic of the NICI Instrument

The key instrument elements are**:**

a. An Integrated, Coronagraph Optimized Adaptive Optics (AO) system. The role of this system is to concentrate the energy from sources in the smallest possible area so that it is more visible and picks up less background

b. Dual channel camera. This camera is the "heart" of the instrument. By making simultaneous, dual beam differential observations, we will reach new levels in background removal.

c. Low scatter, Ghost-Free Optics. The all-reflective optical train is designed to minimize the number of surfaces and eliminate ghosts.

d. Dual 1024x1024 InSb Detectors. One detector per channel operating over the 1-5 micron with range with high density sampling – 0.018 arcsec/pixel.

e. Mask, Dichroic and Filter wheels. Allow a choice of spectral and coronagraphic options

Functionally, the instrument takes light from the telescope focus and relays it onto the deformable mirror where atmospheric phase errors are corrected (AO Relay). Light is then relayed onto the first instrument focal plane where one of several coronagraphic masks can be selected. There is a dichroic in the AO Relay that strips off the visible wavelength light and sends it through the AO Bench to the Wavefront Sensor(WFS). The beam enters the dewar and is collimated. An image of the pupil is formed downstream of the collimator. At the reimaged pupil, the collimated beam is masked by a choice of pupil masks, applying a variety of coronagraphic strategies.

The masked, collimated beam is then split into two beams by a number of different strategies at the dichroic wheel. This beam division could involve dichroics, filters, neutral splits, or polarizing elements. Each of these beams is sent to an essentially identical camera. Each channel has its own selectable filter wheel to further define the beam properties. Each of the two beams is then reimaged onto a detector. In one channel, an extra, selectable optic allows imaging of the pupil for diagnostic purposes.

The goal of the two-channel camera is to obtain images that have undergone the same atmospheric turbulence history. By finding a two channel split in which the source to background ratio varies significantly, we can isolate the source light by differencing, since one channel is always estimating the background. Between the focal plane and pupil plane mask choices, the beam division choices, and the separate filter wheels in each channel, there are literally thousands of instrument configurations possible.

4.2. Overview of the NICI Instrument

NICI is mounted at the Cassegrain focus of the telescope, preferably in the bottom or up-looking position, since this minimizes the number of surfaces between the instrument and the sky. The first instrument subsystem, the Adaptive Optics (AO) relay, images the telescope focal plane (TFP) on to the first instrument focal plane (IFP1). It consists of a pair of off-axis parabolic mirrors (OAPs), an 85 element deformable mirror (DM), a visible transmitting/IR reflecting dichroic and one flat fold mirror. The first OAP images the telescope entrance pupil onto the first instrument pupil plane (IPP1) where the deformable mirror (DM) is located. The DM reduces atmospheric phase errors based on phase information generated in the AO wave front sensor (WFS). Following the DM, a second OAP relays a corrected, real image of the telescope focal plane to the first instrument focal plane (IFP1) located just above the window of the cryostat. The visible wavelength light is separated by the dichroic and sent to the WFS off a fold mirror. The infrared light is reflected out of the plane of the paper to the cryostat.

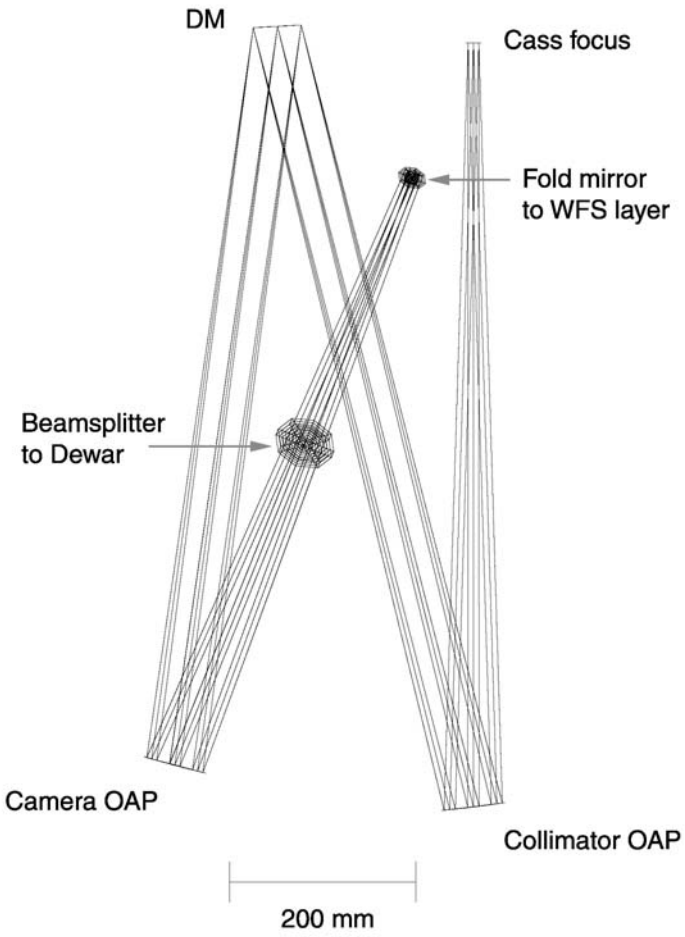

NICI Adaptive Optics Relay Optical Layout

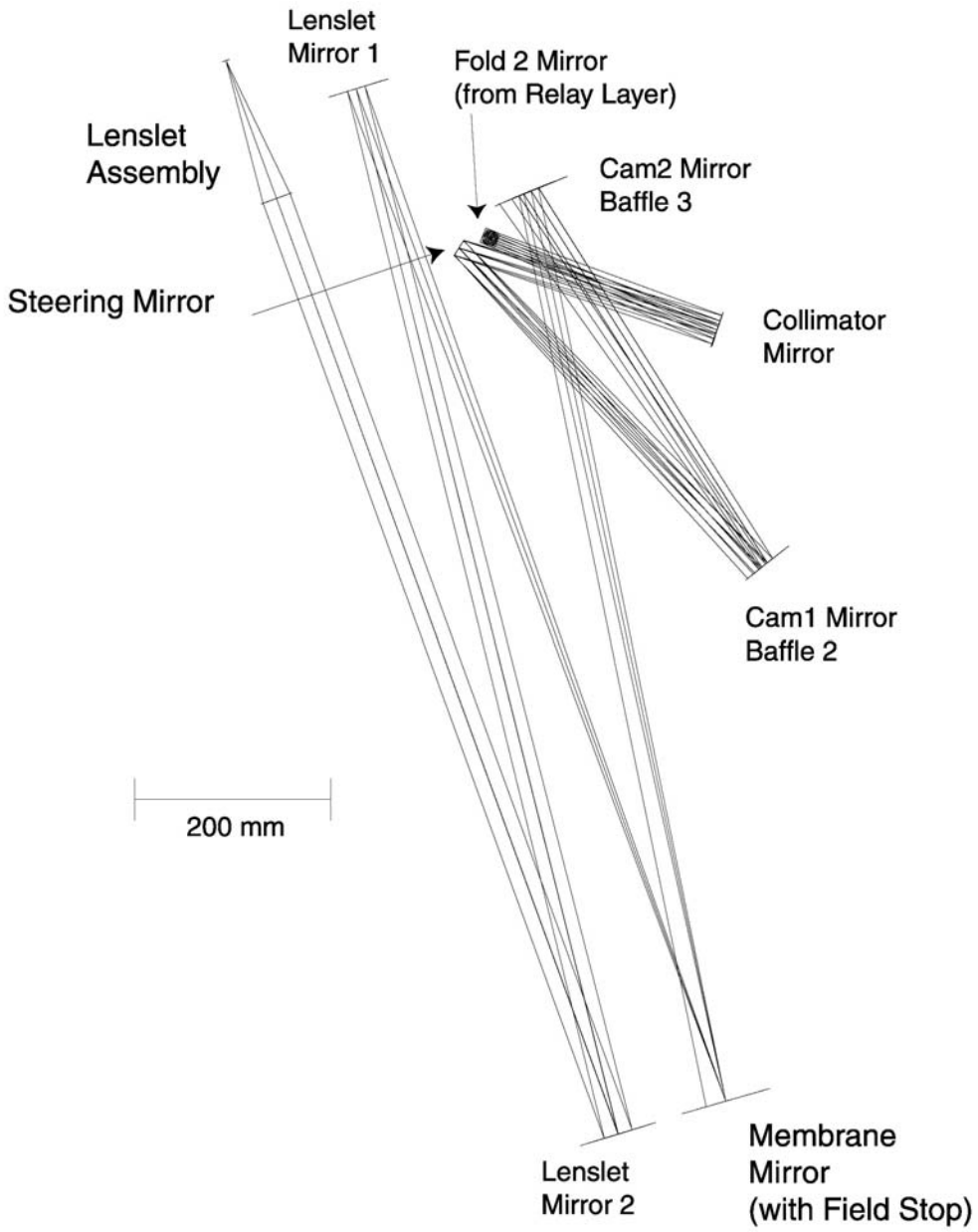

NICI Adaptive Optics Wavefront Sensor Optical Layout

The wavefront sensor(WFS) elements are located on the back of the same optical bench that mounts the AO Relay. The job of the WFS is to form an image of the entrance pupil on a steering mirror that is used to adjust the boresight of the IR camera to the WFS center. The steering mirror is also needed to allow dithering and atmospheric refraction correction. The WFS optics must also form a focal plane image at f/60 on the membrane mirror. The membrane mirror scans focus of the WFS plus and minus at about 2 kHz. Finally the WFS optics reimage the entrance pupil on the lenslette array. The purpose of the WFS is to measure two out of focus images at 2 Khz for from which the wavefront errors will be computed.

The Infrared beam, or science beam, is reflected off of the dichroic in the AO Relay, normal to the AO bench towards the IR Camera. The IR Camera is a reimager with about a factor of 2.5 magnification with a dichroic split, two filters wheels and two detectors that will give simultaneous images at two wavelengths. The focal plane reimaged by the AO Relay falls a couple of centimeters in front of the Camera/cryostat window. At this focal plane position is located a wheel with 8 coronagraphic masks. These will be apodized masks on a calcium fluoride substrate. The Camera optics consist of a simple all-reflective two off-axis parabola design with two fold mirrors to isolate the pupil reimaged by the first parabola. With the exception of the pupil imaging lens all of the mechanisms are located at or near the pupil plane between the two fold mirrors. The first mechanism is a spider mask that will reduce the spider flares in the final image plane. This mask must be rotated as the instrument rotator de-rotates the image. This is followed by the pupil plane mask wheel with a selection of 8 undersized pupil plane masks. The next mechanism is the dichroic wheel that provides a selection of 15 beamsplitting options. Following the dichroic are two identical channels each with a 22 element filter wheel and a parabola to image onto the 1024x1024 1-5 micron Aladdin style array with a plate scale of 0.18 arcseconds/pixel.

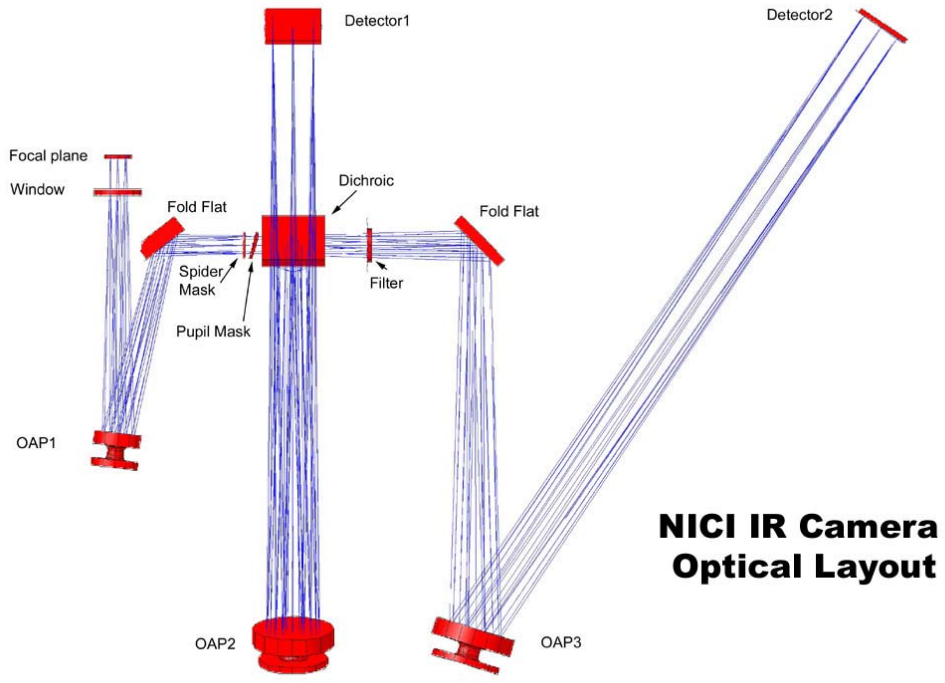

4.3. Description of Mechanisms

NICI has 13 mechanisms that will be controlled by the Observer to configure the instrument for a given observation. The table below lists the mechanisms. A brief description of each follows.

Mechanism	# of Positions	Type of drive
AO Relay		
Fiber optic calibration sources	4	Four position translator
Wavefront Sensor		
Tip/tilt steering mirror	continuous	Two angle tilt mirror
Neutral density filter wheel	6	Discrete position wheel
Cryostat		
Focal Plane Mask wheel	8	Continuous rotary wheel
Spider Mask Rotator	continuous	Continuous rotary drive
Pupil Mask Wheel	8	Discrete position wheel
Beam splitter/dichroic wheel	15	Discrete position wheel
Channel 1 filter wheel	22	Discrete position wheel
Channel 2 filter wheel	22	Discrete position wheel
Pupil imaging optics	3	Discrete position wheel

Fiber optic calibration sources - This translator has four positions. Position 1 will have a single mode fiber mounted at the Gemini cassegrain focus position and will be used for systems tests and adaptive optics calibration. The second position will have a 5x5 grid of single mode fibers at the Gemini cassegrain focus position and will be used for calibration of distortion and for mapping one detector to the other. The third position will have two fibers located in opposite corners of the field of view. These two fibers can be used while take a science image and will produce two adjustable brightness images in the corners of the arrays and will be used to track registration of the two arrays. The fourth position is the open position. This mechanism will also function as a dust cover by closing the optical path when position 1 is selected. Position 1 is the home position.

Tip/tilt steering mirror – A steering mirror is required to adjust the boresight of the AO system with respect to the IR Camera. An example would be to position the

guide star at the edge of the frame. This mechanism is a tip/tilt, or two angle, mirror that is used to center the star image in the wavefront sensor 5 arcsecond field of view. This mirror will be adjusted when dithering more than 2 arcseconds or when guiding on an off axis object. It will allow guiding over the entire 18 arcsecond diameter field. It will also be used to correct atmospheric refraction.

Neutral density filter wheel - The brightness of the guide objects will range from extremely bright to very faint. This wheel will be equipped with an ND3 and an ND4 neutral density filter to reduce the guide star flux to levels appropriate for the avalanche photodiodes in the wavefront sensor. A red filter will also be included to improve signal to noise on reddish guide objects when the moon is up. This wheel has 6 positions. The home position will be a blank-off.

Focal Plane Mask wheel - The observer will be able to choose from one of eight focal plane masks. One of the focal plane mask positions will provide a calibration mask. Four positions will provide standard stellar masks of different sizes. One position will be used for the grism slit, and the remaining positions will be for observer supplied masks. The mask will be selected by positioning the wheel to the correct position for the selected mask. One dimensional dithering is then accomplished by small movements of the wheel.

Spider Mask Rotator - The spider mask is a cross shaped mask that aligns with the spider image in the cryostat. The mask must be rotated to stay aligned with the telescope spiders when the instrument rotates to de-rotate the field. The alignment of the spider mask will be automatic. Once the observer selects that the spider mask mechanism is active, it will track the telescope rotator position and position itself accordingly. It will repeat this process every 60 seconds to maintain alignment.

Pupil Mask Wheel - The pupil mask wheel allows the selection of a pupil plane mask from a choice of eight masks. The pupil plane mask stops down the outer edge and inner edge of the image of the secondary. For instance, the outer edge maybe stopped down to 90% of the full telescope pupil image. A similar area is masked around the inner hole. As the focal plane mask gets smaller the pupil plane mask needs to be more restrictive. Four of these masks will be sized to cover the range of focal plane mask sizes. The other positions will be used for special purpose masks such an apodized pupil mask or a grism.

Beam splitter/dichroic wheel - This wheel has 15 positions that determine which wavelengths are sent to each channel. Different experiments will require that the beamsplitting wavelength change. The table below shows the planned population of the beam splitter/dichroic wheel. The project budget for these elements is $64,000 so it will not be possible to fully populate this wheel.

Channel Splitting Elements – Dichroics			
	Channel 1 Response	**Channel 2 Response**	**Name**
Position #1	< 1.8 microns	> 1.9 microns	H/K
Position #2	< 4.2 microns	> 4.4 microns	L/M
Position # 3	1.2-1.4 microns	1.4-1.7 microns	H Methane
Position #4	2.0-2.15 microns	2.15-2.3 microns	K Methane
Position #5	< 3.6 microns	>3.7 microns	L- Methane
Neutral Density Elements			
	Channel 1 Response	**Channel 2 Response**	**Name**
Position #6	50% 1.0-2.4 microns	50% 1.0-2.4 microns	50/50 Short
Position #7	50% 3.3-4.9 microns	50% 3.3-4.9 microns	50/50 Long
Calibration/Maintenance Elements			
	Channel 1Response	**Channel2 Response**	**Name**
Position # 8	100%	0.	Hole
Position # 9	0%	100%	Mirror
Line/Continuum Elements			
	Channel 1 Response	**Channel 2 Response**	**Name**
Position #10	1.6 microns	Continuum	Methane
Position #11	1.64 microns	Continuum	[FeII]
Position #12	2.122 microns	Continuum	H2 1-0 s (1)
Position #13	2.166 microns	Continuum	BracketGamma

Position #14	Spare(open until used)		
Position #15	Spare(blank until used)		

Channel 1 filter and Channel 2 filter wheels - Each channel will have a filter wheel with 22 filter locations. Since each wheel will have a blank position there will be 21 available filter locations. Since the 50/50 beam splitters allow the reversing of the long and short channels, the initial complement of filters will be nearly the same in each wheel. The table below lists the layout for each wheel. The planned initial complement of filters that will be shipped with the instrument are indicated with a *. The filter budget for the project is $45k. Filters at the other locations will be added by Gemini at a later time.

Filter Position #	Channel 1 Wheel	Initial Complement	Channel 2 Wheel	Initial Complement
1	Blank-off	*	Blank-off	*
2	J	*	J	*
3	H	*	H	*
4	K'	*	K'	*
5	L'	*	L'	*
6	M'	*	M'	*
7	H methane on		H methane on	
8	H methane off		H methane off	
9	K methane on	*	K methane on	*
10	K methane off	*	K methane off	*
11	L methane on		L methane on	
12	L methane off		L methane off	
13	J age filter 1		J age filter 1	
14	J age filter 2		J age filter 2	
15	[FeII]		[FeII]	
16	[FeII] cont.		[FeII] cont.	
17	H2 1-0 s(1)	*	H2 1-0 s(1)	*

18	H2 1-0 s(1) cont.	*	H2 1-0 s(1) cont.	*
19	Br gamma	*	Br gamma	*
20	Br gamma cont.	*	Br gamma cont.	*
21	Grism 1		Grism 3	
22	Grism 2		Grism 4	

Pupil imaging mechanism - Pupil imaging, that is forming an image of the telescope entrance pupil on the array is required in NICI. There is no better diagnostic of coronagraph performance than a pupil image and no more effective tool to align the Lyot stop and spider mask. The pupil imaging mode will also be used initially to understand the alignment and flexure of NICI on Gemini, and will provide crucial data on the state of the telescope by showing the distribution of light at the pupil mask. . The pupil imaging optics should be independent, and the science optics must not move when going into pupil imaging mode.

A pupil imaging mode has been included as a diagnostic function. Using the pupil imager will allow the alignment of NICI with the telescope to be checked as well as the alignment of the pupil plane mask, spider mask filters, and dichroic wheel. Normally the observer will not use the pupil imager for typical science projects. This wheel has three positions, open, blank-off and pupil image. The pupil image is about 200 pixels across.

4.4. NICI Electronics Overview

The control electronics for NICI is comprised of two largely independent systems. One handles the array and mechanism control and the other the AO system. These electronics are housed in two Gemini cooled enclosures and one auxiliary cabinet for the AO system APDs. The diagram below shows the layout of the two cabinets.

Electronics Box Layout

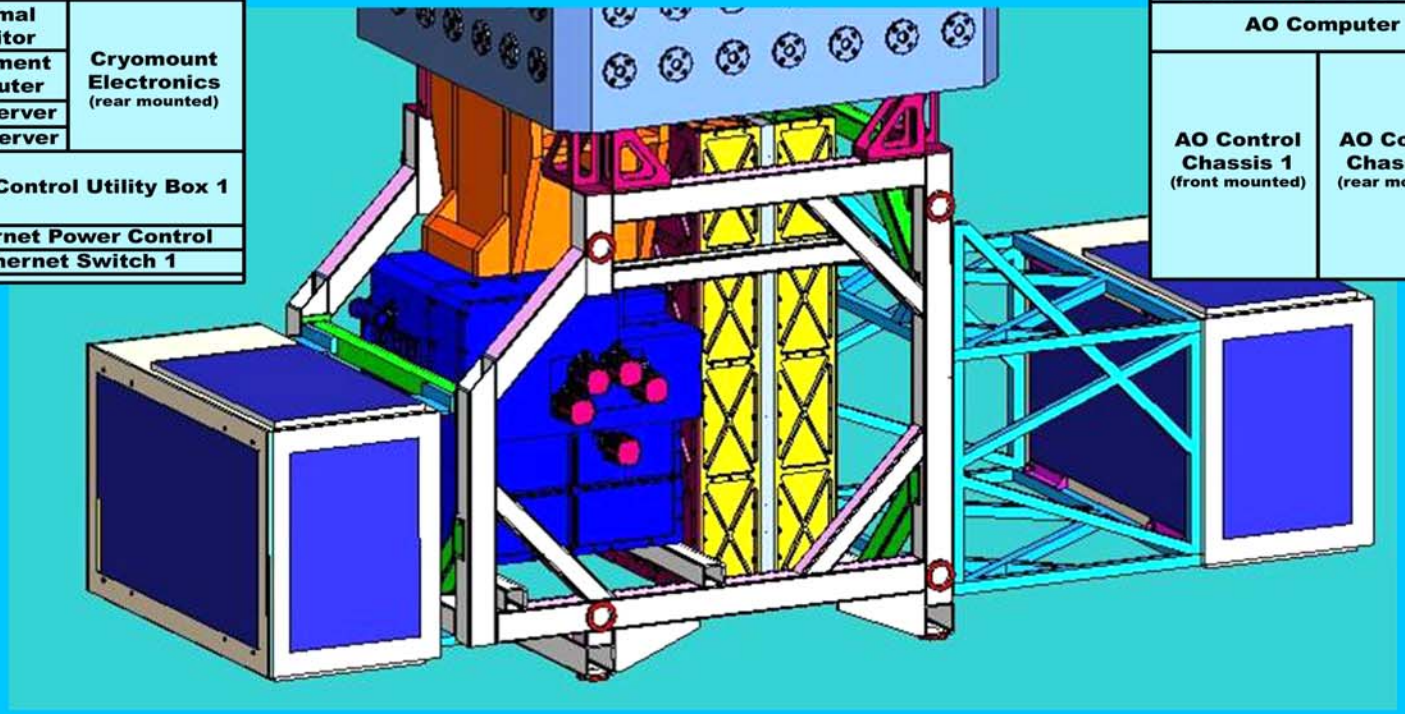

Array and Mechanism Control Overview

The hardware for control of the two infrared arrays and the mechanisms for the cryostat and AO system is shown on the block diagram on the following page. The Instrument Control Computer is the prime controller for the entire instrument. It will receive commands from the instrument sequencer and orchestrate actions of each of the sub-systems. When an array operation is requested the Instrument Control Computer will setup the array clockers, pixel servers and provide instructions for the data handling. Communications with the temperature controller and mechanisms is a serial server in the utility box.

Array Control

The analog portion of the array control is done by the cryostat electronics which contains the preamplifiers, clock level shifters and A/Ds. The Cryostat Electronics also contains the clocker, a small PowerPC/FPGA board that is Ethernet controlled. An image is initiated by the Instrument Control Computer which loads or selects the appropriate readout clock pattern into the clocker. As the array is clocked the data is passed through the preamplifiers and then sampled by the 16 bit A/D converters. The data is sent back to the pixel servers via a commercial fiber system. The pixel servers have also received instructions from the Instrument Control Computer as to how much data to expect and what is to be done with it.

Mechanism and temperature control

The mechanism are primarily serially controlled Animatics Smartmotors. The Smartmotors have limit switch inputs on the motors and are capable of local operations such as go to home or move a number of steps. The serial connections are made through a terminal server in the utility box.

Temperature control is done using three commercial temperature controllers. Two are servo controllers used to maintain the detector temperatures. The third is an eight channel temperature monitoring that will provide information about the health of the cooling system for the cryostat.

Ethernet Power Control

Ac power to each electronics box can be turned on or off remotely to facilitate remote troubleshooting.

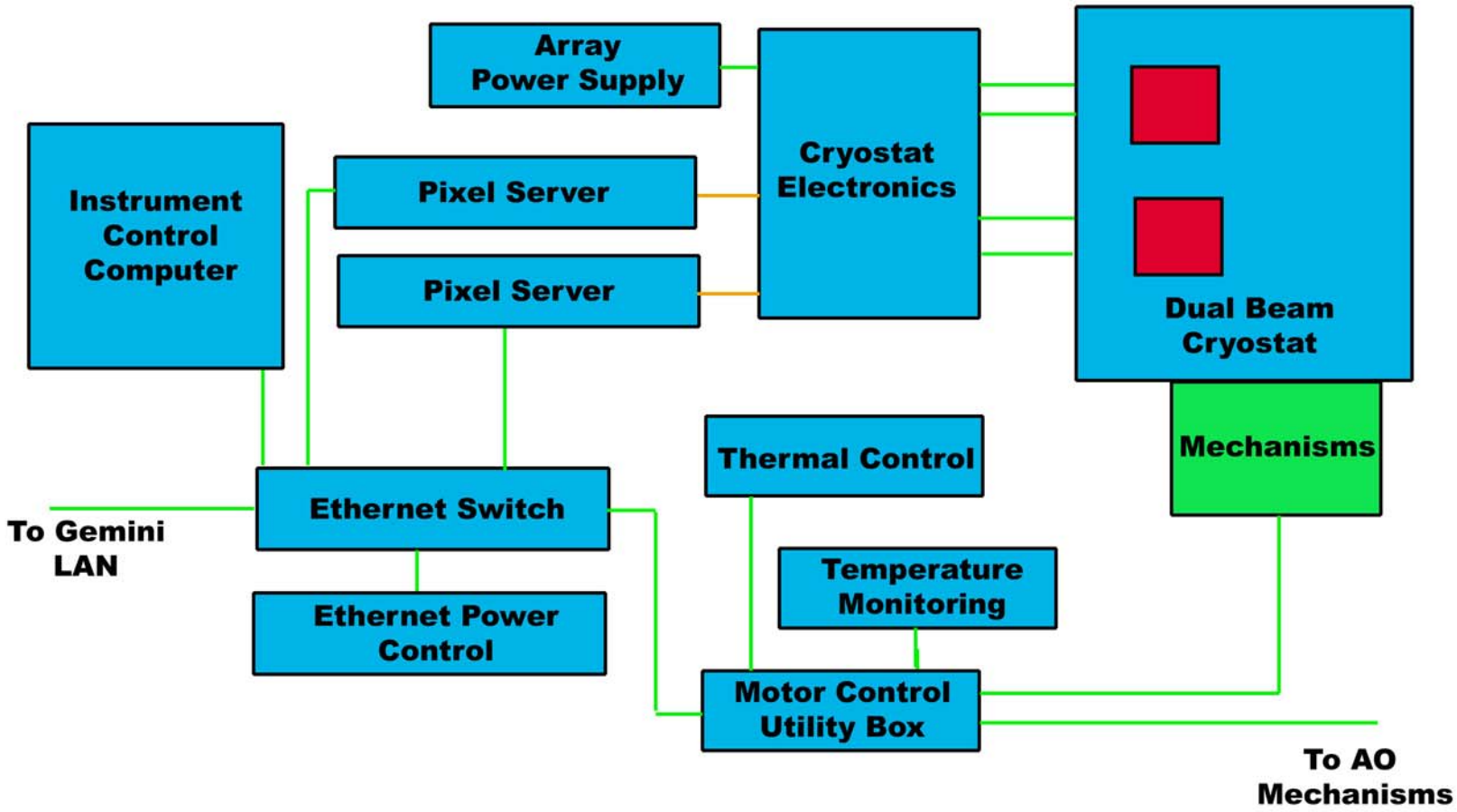
Array
Power Supply
Cryostat
Electronics
Dual Beam
Cryostat
Instrument
Control
Computer
Pixel Server
Pixel Server
Mechanisms
Thermal Control
Ethernet Switch
To Gemini
LAN
Temperature
Monitoring
Ethernet Power
Control
Motor Control
Utility Box
To AO
Mechanisms

Adaptive Optics Electronics Overview

The Adaptive Optics controller is a largely independent sub-system. It has its own control computer that receives instructions from the Instrument Control Computer via the Ethernet switch. The AO control loop starts with the lenslette array on the AO bench. The two out of focus images are measured and the light fed via fiber to the APD modules. The counts out of the APD modules go to the AO Control Chassis into gated counters. This data is then sent via fiber to the AO control computer which does the loop calculations and sends the deformable mirror voltage data back to the AO Control Chassis via fiber. This data is then sent to the high voltage amplifiers and on to the deformable mirror. The controller in the AO Control Chassis also creates the control signal for the membrane mirror.

The following observer functions will be supported by the AO software:

AO on/off	Turn on or off the AO corrections
Steering Mirror Adjust	Tip or tilt the steering mirror to maximize signal
Membrane Mirror Throw	Adjust the amount of throw on the membrane mirror
ND Filter Control	Select an ND filter
Servo Parameters	Adjust the AO loop parameters

To Lan
AO Power Supplies
AO Control Chassis 1
AO Control Chassis 2
AO Control Computer
Ethernet Switch
Ethernet Power Control
APDs
APD Power Supplies
AO Utility Box
AO Bench

4.5 Software Overview

The NICI software is comprised of many modules operating on many different processors. External control is via Ethernet and allows multiple clients to allow remote support and troubleshooting. The Instrument Control Computer is the master controller of the instrument. It controls array operations, communicates with the Adaptive Optics System and commands the mechanisms and temperature systems. All control is through this computer. The block diagram below shows the top level view of the NICI software.

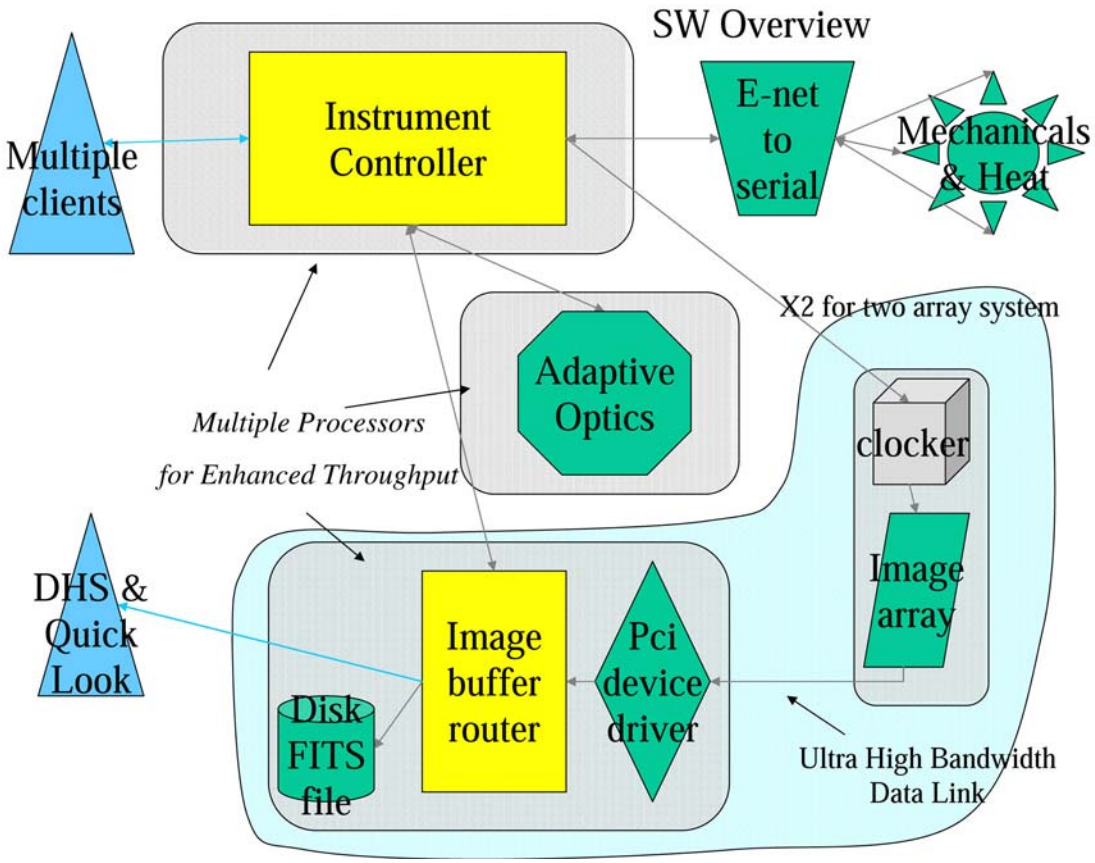

Details of the software can be found in the following documents:

SDN 1005	NICI Mechanism Interactions and Interlocks
SDN 4002	NICI Mechanism Control
SDN 4003	NICI Temperature Control Software
SDN 4004	The NICI to DHS Interface
SDN 4005	Software Array Control and Image Acquisition for the NICI instrument

SDN 4001	NICI Software Overview
IS/IC ICD	Instrument Sequencer to NICI Instrument Controller ICD
IC/AO ICD	NICI Instrument Controller to AO Controller ICD

5.0 Observer Operations

5.1 Overview

The scientific projects that will be addressed with NICI will vary greatly in scope. The core science projects, however can be represented by a small group of Observing Scenarios that will be described in detail later in this section. These observing scenarios will be used to explore in detail how NICI will work and how an Observer will use NICI. The scenarios will start with setup and calibration procedures. Next will be the "kitchen sink scenario" which will be a very extensive and detailed treatment of a typical differential observation with dithering and atmospheric refraction correction. Finally special cases will be discussed.

5.2 Setup and Calibration

5.2.1 Pre-Run Planning setup

Select a list of science objects

Find stars for PWFS using the Gemini Observing Tool

Determine a sky position that can use the PWFS probe science position

Determine if the central star is sufficient for IAO use

Determine ND filter need for OIWFS

Deselect objects that have poor guide options from list

Select Focal plane mask, Pupil mask, Dichroic, Filter 1 and Filter 2 for each observation

Daytime Setup/checkout

Camera calibration/checkout

Select the chosen Pupil mask 90:10

Select focal plane mask - open

Select the chosen Dichroic Short 50/50

Select Filter channel 1 - J

Select Filter channel 2 - J

Select the fiber calibration source - grid

Select fiber brightness

Set the integration parameters

Set comment field to mapping calibration

Take and save mapping calibration image with both arrays

Determine offset and rotation for quick look parameters

Select focal plane mask - .3 arcsec

Select Dichroic – Long 50/50

Select Filter channel 1 – L'

Select Filter channel 2 – L'

Set integration parameters

Set comment field to mask location

Take and save mask location images with both arrays

Determine position of center of the mask

AO calibration/checkout

Select ND filter wheel position – ND4

Select fiber calibration source – single fiber

Set fiber brightness

Set steering mirror to home position

Set offload AO focus tertiary– off

Set offload AO tilt tertiary - off

Check APD counts

Set AO loop – on

Select the chosen Pupil mask - open

Select focal plane mask - open

Select the chosen Dichroic Short 50/50

Select Filter channel 1 - J

Select Filter channel 2 - J

Set integration parameters

Set comment field to boresight

Take and save boresight images with both arrays

Determine position of fiber source image and compare to center of mask

Adjust steering mirror to put source image on center of mask pixel

Record nominal center position for the steering mirror

Calibration

Night-time Calibration

In between science objects, and for each setting of filters or dichroics, the facility calibration unit will be used to take flat fields. These will be used in addition to the sky flats until the optimal field flattening is determined.

Flats with Facility Calibration Unit

Pause IAO

Select Facility calibration unit – Black body mode

Set integration parameters

Set comment field to flat

Take and save flat science image both channels

Set integration parameters for 2 times xxx seconds and 10 coadds

Take and save flat science image both channels

Twilight Setup

Slew to sky position near science object

Position PWFS probe for the selected star

Set instrument rotator at 0 degree position angle

Set instrument rotator to de-rotate image

Set spider mask rotator to active

Select the Pupil imager mode

Select Filter L in channel 2

Set .1 sec. integration time and 1 coadd

Set comment field to spider mask

Take a setup image to check pupil mask and spider mask alignment

Verify spider mask position covers spiders and adjust if required

Deselect pupil imaging mode

Slew to science object

Reacquire stars for PWFS

Command OIWFS steering mirror to nominal center position

Select OIWFS ND filter for guide star

Set channel 2 filter back to science filter

Activate IAO system with default parameters

Take channel 1 image and send to DHS for centering analysis

Offset OIWFS steering mirror according to result from DHS process

Record OIWFS spatial zero points and set new nominal center position

Determine and set optimal IAO servo parameters

Take image with channel 1 to view spider flares

Adjust spider mask zero point to minimize spider flares

Set new spider mask zero point

Sky flats:

Pause IAO

Offset to sky position – reacquire guide star with PWFS2

Set integration time to xxx seconds coadds to 10

Select simultaneous integration mode

Set comment field to sky flat

Take and save sky frames

Dither position and repeat x times

Verify on quick look display that no stars are present in sky field

5.3 Science Observations

The procedures for the science observations will vary with the type of observing project being executed. The procedures listed below describe the process for each of the following observing scenarios:

Spectral Differential Imaging with Dithering and Grism followup

Point Spread Function Differencing with Dithering

Photometry of a Faint Companion

5.3.1 Spectral Differential Imaging with Dithering and Grism followup

Differential imaging is certainly not new to infrared astronomy. Traditional beam switching and sky subtraction is a differential imaging method. The difference with NICI will be that the differential imaging will be simultaneous, and that the difference will be between images at two wavelengths. This reduces the importance of the sky images, which will now be used as a processing aid, and at times for a flat field. Objects will typically be stared at for long periods of time (up to 2 hours) and sky frames taken about 10% of the time.

Dithering is also a bit different with NICI. Typically, observers will dither in a two dimensional pattern with steps of 2-5 arcseconds or more. NICI has such a small field that a plus and minus five arcsecond dither would throw away about half of the field. With NICI, the dithers will be small. Typical dithers will be about an arcsecond. Additionally, the dithers will be in an arc as defined by the rotation of the focal plane mask wheel. This is in a sense a 1 dimensional dither.

Examples of the projects this type of observing method would be used for are: methane companion searches, brown dwarf age measurements, and imaging of ionized outflows from YSOs.

The Adaptive Optics system will have an algorithm that will set or recommend the values for membrane mirror throw and AO loop gain.

The following is a typical observing sequence for Differential Imaging with Dithering where a source is found and follow up spectra is taken with the grism mode. This is the "kitchen sink" scenario and will exercise every aspect of the instrument.

Setup Prior to Observation

Fiber Calibration Slide to corner fiber position

Camera Pupil Wheel to blank

Set ND filter to blank

Set steering mirror to nominal center position

Set PWFS to guide star position

Slew telescope to science object

Acquire star with PWFS

Set ND filter for guide star brightness

Check for adequate APD counts

Set membrane mirror throw

Set AO loop gain

Turn AO loop on

Set Tip/tilt offload on

Set focus offload on

Select focal plane mask – .3 arcsec

Select the chosen Dichroic K methane

Select Filter channel 1 – K methane on

Select Filter channel 2 – K methane off

Set pupil imager to open

Set low array bias

Set integration time

Set other array parameters

Set coadds

Set simultaneous read mode to channel one only

Set comment field to "science object name"

Select desired sky rotation and command OCS to de-rotate image

Set spider mask rotator to track on

Set pupil mask wheel to 90:10

Set DHS destination to quicklook

Take a frame channel 1

SSA to adjust centering if required

Repeat take frame until centered

Set atmospheric refraction correction to on

Set simultaneous read mode to both channels

Ready to take data

Take science frames (~5 frames 60 seconds each=~5 minutes)

Save frames to DHS and send to quick look

Dither to position #2

Move OIWFS steering mirror, focal plane mask and PWFS probe to desired dither amount in a simultaneous move

Take science frames (~5 minutes)

Dither to position #3

Take science frames (~5 minutes)

Dither to position #4

Take science frames (~5 minutes)

Dither to position #5

Take science frames (~5 minutes)

Dither to position #6

Take sky frames

Set the AO loop to pause

Offset to sky position

Set integration time

Set comment field to sky

Offset telescope to sky position

Take sky frames (5 minutes)

Return to science object position

Reaquire guide star with PWFS

Set AO loop to on

Set integration time

Repeat Dither sequence on object and sky 3 more times

Flats with Facility Calibration Unit

Pause AO

Select Facility calibration unit – Black body mode

Set integration time x seconds for flat

Set comment field to flat

Set DHS destination to quick look

Take flat science image both channels

SSA verify levels correct for flats on quick look

SSA adjust integration time if required

Set coadds to 10

Set DHS destination to save and quicklook

Take flat science image both channels

Set integration time to 2x

Take flat science image both channels

Grism Follow up

A very important design goal of NICI is the ability to measure a low to medium resolution spectrum of faint objects. Objects detected by spectral differencing will require at least a low resolution spectrum to allow classification of the object. Objects detected near the detection limit of NICI will be very difficult to follow up on other telescopes with other instruments.

NICI will greatly reduce the light from the central star, but there may still be a significant halo that will contaminate the spectrum of the companion. The observing technique must allow for the measurement of the spectrum of the residual halo around the companion so that it can be subtracted from the companion spectrum. Since for most cases the slit will have to be positioned along the parallactic angle, radial or tangential orientations of the slit with respect to the system understudy will not usually be possible. Typically dithering along the slit is done with this type of measurement and will be included in this scenario.

Assume that a companion is seen in the field around the target primary. The following sequence would be used to take a grism spectra. The focal plane mask must be changed to the slit mask. The slit mask has two slits of different widths. One is south of the center oriented north/south and the other is north of the center also oriented north south. If the grism mode selected spans much wavelength range the atmospheric refraction will smear the image larger than the slit width. The slit must therefore be positioned so that it is oriented along the parallactic angle so that the smear is along the slit. This positioning is done with the instrument rotator. Since the grisms are located in the filter wheel two grisms can be used simultaneously. Therefore in addition to the slit the dichroic must be selected and the grisms selected in each filter wheel. This scenario continues assumes that the previous sequence was just completed and that a companion was found. The AO system is still locked onto the primary.

Measure the companion's position with respect to the primary
Calculate the current parallactic angle of the companiton
Offset the rotator angle to put the slit on the parallatic angle
Acquire a star in the PWFS and turn on guiding using non-sideral tracking mode
Verify position if integration time to detect companion is short
Set focal plane mask wheel to slit
Set pupil plane mask wheel to grism mask
Set dichroic
Select grisms in channel 1 and channel 2
Set integration time
Set comment field to grism spectrum
Take and save science frames
Move steering mirror to dither position along the slit
Repeat science frames and dither positions.
Set AO loop to pause
Set atmospheric refraction correction to off
Offset to sky position
Set integration time
Set comment field to "grism sky"
Take and save science frames
Dither position and repeat science frames
Offset telescope to standard star position
Reposition instrument rotator to put slit on parallacctic angle for standard star
Acquire guide star with PWFS and begin tracking in no-sidereal mode
Adjust WFS ND filter if required
Set AO loop to on
Using the steering mirror position star in slit
    Remove slit and image if needed
Set integration times
Set comment field to grism standard #
Take and save science frames
Dither position along the slit and repeat science frames

5.3.2 Point Spread Function Differencing

When there is no reasonable spectral feature that allows the spectral differencing mode to be used images will be taken in two filters such as H and K, or L and M, and then differenced with a nearby reference star. While a less sensitive and less powerful observing mode than the simultaneous modes, this will still be important observing mode. A typical project would be the imaging of optically thick disks around other stars. The dusty disks have no strong spectral features. That allows the cancellation of the residual stellar light, and must be differenced with a sequentially observed star to remove the residual halo, leaving only the light from the disk.

Best results are achieved with a reference star that has no known infrared excess, that is similar brightness and color to the target star, and is very close to the target star. The telescope will be offset between the two stars on a time scale that is short enough to allow the PSF to be similar and long enough not to drastically impact the integration duty cycle. Typical switching times would be on the order of five minutes over a period of two hours, resulting in 24 pairs. Each pair may be comprised of up to five images of each object, for a total of 240 images.

Sky frames will be taken about ten percent of the time to be used in data reduction. Sky frames from the whole night or run are combined to produce a flat.

This scenario assumes that the Setup Prior To Observation sequence in 5.2.1 is just complete. This means that the star is centered on the mask and the AO loop is on and locked on the guide star. The spider mask position is active and atmospheric refraction correction is on. For this experiment the .15 arcsecond focal plane mask, 85:15 pupil mask, K/L dichroic and channel one filter K and channel 2 filter L' are selected.

For this observing the target star and reference star will be imaged alternately with a cadence that is a balance between minimizing changes in the PSF and conditions and observing efficiency. The integration time should be at least equal to the overhead time to transit between stars and set up. Usually integrations are at least 5-10 minutes.

Set simultaneous mode to both channels asynchronous

Set independent integration times

Adjust coadds to yield same total integration times

Set comment field to science object name

Take and save science frames

Set AO loop to pause

Set PWFS to position for reference star

Offset to reference star

Acquire guide star with PWFS

Set AO loop to on

Adjust integration times if required

Set comment field to Reference object #####

Take and save science frames

Dither position with steering mirror offset and repeat

Set AO loop to pause

Set PWFS to position for the science object

Reset integration times if changed for reference

Offset telescope to science object

Reacquire guide star with PWFS

Turn AO loop to on

Repeat science frames offsetting between objects

Offset to sky every 5 cycles and take a sky sequence

Before and or after full sequence take flat frames as above.

5.3.3 Photometry of a Faint Companion with Dithering

The discovery mode of NICI will be very powerful for finding new objects to study but this mode represents only the start of the real science. Merely finding a faint object or extension next to a star is not enough. Quantities must be measured about the discovery in order to make meaningful progress toward understanding these systems. Accurate spectra and photometry are crucial for this progress.

Photometry of a faint companion is similar to traditional photometry except that the dominant background is not from the sky or the telescope but from the parent or central star. As with the spectral mode the observing technique must enable the removal of the residual background from the star so as not to corrupt the photometry.

Since this observing mode is not a differential mode, sky frames will be taken in the normal fashion.

This scenario assumes that the Setup Prior To Observation sequence in 5.2.1 is just complete. This means that the Science object is centered on the mask and the AO loop is on and locked on the guide star. The spider mask position is active and atmospheric refraction correction is on. For this experiment the .3 arcsecond focal plane mask, 90:10 pupil mask, H/K dichroic and channel one filter H and channel 2 filter K are selected. Instrument rotator is derotating image.

Set Channel one and channel two integration times and coadds

Set comment field to science object name

Take and save science frames (60 sec)

Set AO loop to pause
Set comment field to sky position
Offset to sky position
Take and save sky frames (60 sec)
Offset to science object
Set comment field to science object name
Take and save science frames
Repeat Object/Sky pairs 5 times
Dither the position
Move OIWFS steering mirror desired dither amount
Move focal plane mask same amount
Take and save science frames (60 sec)
Offset to sky position
Take and save sky frames (60 sec)
Offset to science object
Repeat Object/Sky pairs 5 times
Repeat dither 3 more times
Change filters and repeat if more wavelengths are required

Set AO loop to pause
Offset to flux standard position
Reposition PWFS for Flux standard
Set AO loop to on
Position star on the same starting pixels as the companion
Take science frames (60 sec)
Offset to sky position
Take sky frames (60 sec)
Offset to science object
Repeat Object/Sky pair 5 times
Dither the position
Take science frames (60 sec)
Offset to sky position (use PWFS1 for primary corrections)
Take sky frames (60 sec)
Offset to science object (use PWFS1&2 for Primary corrections)

Repeat Object/Sky pair 5 times

Repeat dither 3 more times

Change filters and repeat if more wavelengths are required

Other flux standards and extinction stars will be done in the same way as the flux standard above. Flat fields would be taken by preferred method or made from stacking up the sky images.

5.3.4 Astrometry

Prime among the NICI science objectives is discovering new companions. Yet the sensitivity limits achievable with NICI are deep enough that often faint detections will be background objects. It is important that an accurate position of the candidate companion be recorded so that follow up work can be done to classify the object and to verify that it is associated with the primary star under investigation.

There are a variety of reasons for wanting to know the candidate companion's position and each has a required accuracy. One key reason for wanting the position would be to allow a follow up spectroscopy measurement. Here the desired accuracy would be a fraction of the spectrograph slit, say around 0.1 arcsecond. Another similar reason would be to communicate the position to others so that they could try to duplicate the image. Again around 0.1 arcseconds would be adequate.

A second key reason for wanting the candidate companion's position would be to verify that the companion has the same proper motion as the primary. This is particularly important for objects in large, very slow orbits around the primary. Here the higher the astrometric accuracy the less time is needed to make the measurement. A high proper motion primary would move about a half an arcsecond a year however many target objects would have far less motion. In effect higher astrometric accuracy extends the range of this technique. For this method required accuracy ranges from around a tenth of an arcsecond to as good as you can do.

The third key reason for astrometry is to measure the orbit of the object. A Jupiter orbiting at Jupiters orbit around a star at 5 parsecs will move about 0.5 arcseconds per year. Larger, slower orbits would move far less. Here the accuracy required depends on the science goals and could range from merely proving that the companion is orbiting the primary to looking for detailed information about the orbit and perturbations of the orbit. Again desired accuracies would range from around 0.1 arcseconds to as good as you can get.

What is the practical limit in astrometric accuracy for NICI? Astrometrists prefer an over sampled psf with about 3-4 pixels per FWHM. NICI has 3.5 pixels per diffraction core at K so the sampling is well suited to accurate astrometry. Astrometric telescopes with fat seeing limited psfs are able to centroid to about a few percent of a pixel giving accuracies around a few milliarcseconds. NICI with 18 milliarcsecond pixels should be able to centroid objects to a few milliarcseconds relatively easily. This does not translate to an astrometric accuracy of the same level however.

There are a few challenges with do astrometry with NICI. First there is some focal plane distortion. This is a result of keeping the optics very simple. This distortion is described in SDN1007 Optical Performance. NICI has field distortion as high as 1.8% at the corner of the field. It is much smaller at the center of the field. This would give astrometric errors as high as 0.23 arcseconds at the corner of the field if not corrected. This can be corrected using the ray trace data or by measuring the distortion by moving a star around in the field.

A second challenge for astrometry with NICI is that the psf will not be Gaussian. A high strehl image usually has structure in the PSF. This could cause some centroiding error but is probably offset by the small images and the small pixels.

The primary goal is to achieve astrometric position with respect to the primary and therein lies the largest challenge with NICI. Since NICI occults the primary star and masks the spider flares there is very little light left to process for a centroid. There are four ways listed below to get an accurate position of the primary. Which method is used will depend on the accuracy required and experiments to determine which is most effective. How long it takes to detect the companion will also affect the method used.

Methods to get the centroid of the primary

1)The easiest method is to use the light that spills around the mask, a donut image. This has been used with CoCo on the IRTF to drive the tiptilt system with good results. That was with a seeing limited image that was round and fairly uniform with time. The NICI PSF will have more structure and the structure may change with time this could cause a shift in the centroid. The advantage of this method is that the donut image is always there and can always be used without any extra observational steps.

2) The second and probably best method involves moving the focal plane mask out of the way to image the primary directly. Since the dichroic beamsplitter that feeds the AO WFS is before the focal plane mask the mask can be moved without loosing lock in the AO system. There may be some shift when the mask is moved but this can be checked. The mask does not have to be removed entirely, just shifted enough to get the focal plane mask clear of the star. For very long observations this can be done periodically throughout the observation.

3)The third method would be to intentionally misalign the spider mask periodically. The spider flares point to the primary and can be used for determining the position. This method was also used with CoCo data

4)The forth method would be to use partially transmissive mask. This allows the star to be imaged through the mask at all times. This would probably have to be a hard edge mask since trying to get a centroid of a psf behind a Gaussian shaped transmissive mask would require modeling or characterization measurements to get an accurate position. The hard edged, partially transmissive mask would have degraded coronagraphic performance but would make accurate astrometry easier. The transmission of the mask would have to be tailored to the brightness of the primary being observed. NICI is not baselined to have any partially transmissive hard edged masks but it will have a user position in the focal plane mask wheel where one can be added for special observations.

Using method number 2 astrometric accuracy is expected to be in the 5 milliarcsecond range as long as the distortion is corrected and this method or method 4 is recommended for the highest astrometric accuracy. Method number 1 should yield accuracies of a pixel or less and can be used when accuracy demands are relaxed.

5.4 Data Reduction

NICI will require certain processing algorithms to operate with no human in the loop and for post processing to remove the instrumental signature. The algorithm needed for operation in queue scheduled mode is one to center the star behind the coronagraphic mask.

For operation with a human in control a variety of processing and quick look display algorithms will be needed. The following is a list of the quick look or pipeline processes that will be required. These will be implemented by Gemini and specified by MKIR.

Dual image difference display – This would be a quick look display that will allow the observer to look at the image from both arrays and a difference image that is created using user set parameters for rotation, translation and radial scaling.

Spectral extraction – When used in grism mode NICI will produce two images of the spectral dispersion from the slit. A standard spectral extraction method can be used.

Image registration using corner fibers – When imaging with the corner calibration fibers two spots will be produced in two corners of both arrays. An algorithm will be specified to use these spots for registration.

Calibration using the matrix fiber source – The matrix fiber calibrator will produce 25 spots on each array. An algorithm will be specified to extract rotation, translation and distortion parameters from the data.